Conformational Relaxation and Ligand Binding in Myoglobin

Anjum Ansari,*,‡ Colleen M. Jones,§ Eric R. Henry, James Hofrichter,* and William A. Eaton*

Laboratory of Chemical Physics, Building 5, National Institute of Diabetes and Digestive and Kidney Diseases, National Institutes of Health, Bethesda, Maryland 20892

Received October 4, 1993; Revised Manuscript Received January 13, 1994®

ABSTRACT: Absorption spectroscopy with nanosecond time resolution shows that myoglobin undergoes conformational relaxation on the same time scale as geminate rebinding of carbon monoxide. Ligand rebinding following photodissociation of the heme–CO complex was measured from the amplitude of the average difference spectrum, while conformational changes were measured from changes in the detailed shape of the Soret spectra of the deoxyhemes. Experiments in which the solvent viscosity was varied between 1 and 300 cP and the temperature between 268 and 308 K were analyzed by fitting the multiwavelength kinetic data with both empirical and molecular models. Novel numerical techniques were employed in fitting the data, including the use of singular value decomposition to remove the effects of temperature and solvent on the spectra and of a Monte Carlo method to overcome the multiple minimum problem in searching parameter space. The molecular model is the minimal model that incorporates all of the major features of myoglobin kinetics at ambient temperatures, including a fast and slow rebinding conformation and two geminate states for each conformation. The results of fitting the kinetic data with this model indicate that the geminate-rebinding rates for the two conformations differ by at least a factor of 100. The differences between the spectra of the two conformations generated from the fits are similar to the differences between those of the R and T conformations of hemoglobin. In modeling the data, the dependence of the rates on temperature and viscosity was parametrized using a modification of Kramers theory which includes the contributions of both protein and solvent to the friction. The rate of the transition from the fast to the slow rebinding conformation is found to be inversely proportional to the viscosity when the viscosity exceeds about 30 cP and nearly viscosity independent at low viscosity. The viscosity dependence at high viscosities suggests that the two conformations differ by the global displacement of protein atoms on the proximal side of the heme observed by X-ray crystallography. We suggest that the conformational change observed in our experiments corresponds to the final portion of the nonexponential conformational relaxation recently observed by Anfinrud and co-workers, which begins on a picosecond time scale. Furthermore, extrapolation of our data to temperatures near that of the solvent glass transition suggests that this conformational relaxation may very well be the one postulated by Frauenfelder and co-workers to explain the *decrease* in the rate of geminate rebinding with *increasing* temperature above 180 K.

The binding of ligands by proteins is a fundamental process in biology. One aim of modern biophysical studies is to understand the molecular mechanism of this type of process in detail. There is generally rather little mechanistic information on ligand binding in conventional kinetic studies, such as experiments in which reactants are rapidly mixed. Simple behavior is usually observed, with both the binding and dissociation reactions appearing to take place in a single step. Important information, such as the rate of a conformational change of a protein, can be totally obscured in such experiments. In the case of heme proteins, kinetic studies using flash photolysis have provided a powerful method for investigating conformational changes and the mechanism of ligand binding, revealing them to be complex and interesting processes. The power of the flash photolysis experiment is that photodissociation of the heme–ligand complex produces a coherent population of molecules in which the protein has the conformation of the liganded molecule and the ligand is still inside the protein. The evolution of this unstable intermediate toward the protein conformation of the unliganded molecule, as well as ligand motion and rebinding, can then be monitored by various spectroscopies with time resolution as short as 10^{-13} s. Most studies have focused on myoglobin or hemoglobin because of the considerable amount of X-ray crystallographic information available for these molecules. In particular, the structures of both the unliganded molecules and the molecules liganded with carbon monoxide or oxygen are known at high resolution, so that it is, in principle, possible to relate the kinetics of spectral changes to the kinetics of well-defined structural changes.

New concepts of ligand binding and protein conformational changes relevant to all protein–ligand processes have emerged from the studies on myoglobin and hemoglobin. These include the discovery by Frauenfelder and co-workers of a continuous distribution of protein conformations, so-called "conformational substates", that produce a distribution of geminate-ligand-rebinding rates in solid solutions at low temperature (Austin et al., 1975; Beece et al., 1980; Steinbach et al., 1991) and the discovery of geminate ligand rebinding in liquid solutions at ambient temperatures by Duddell et al. (1979) (Shank et al., 1976; Greene et al., 1978; Alpert et al., 1979; Duddell et al., 1980a,b; Friedman & Lyons, 1980; Chernoff et al., 1980; Cornelius et al., 1981; Catterall et al., 1982; Morris et al., 1982; Hofrichter et al., 1983; Henry et al., 1983a). The work on conformational substates has stimulated the development of analogies between the behavior of proteins

* Correspondance should be addressed to any of these authors.
‡ Present address: Department of Physics, University of Illinois at Chicago, Chicago, IL 60607.
§ Present address: Department of Chemistry, University of South Alabama, Mobile, AL 36688.
® Abstract published in *Advance ACS Abstracts,* March 1, 1994.

0006-2960/94/0433-5128$04.50/0

and other complex systems, such as glasses, spin glasses, and evolutionary trees (Frauenfelder et al., 1991). Geminate rebinding, moreover, is a very general process and occurs in all ligand-dissociation and -binding processes. It is a unimolecular process in which the ligand rebinds to its partner before escaping into the solvent, after which rebinding occurs in a bimolecular process (in bimolecular reactions the geminate complex is called the encounter complex). In heme proteins, geminate rebinding occurs on both picosecond and nanosecond time scales.

One of the major objectives of the photolysis studies on myoglobin, and the principal subject of this paper, has been to develop a detailed molecular mechanism for ligand dissociation and rebinding that also incorporates the protein conformational changes that are known to take place from X-ray crystallography. Although, as we shall see, there has been considerable discussion of this issue, the present work contains the first analysis of the problem, based on direct measurements of the protein conformational kinetics.

The first mechanism to be proposed for ligand binding to myoglobin arose from the pioneering study of Frauenfelder and co-workers (Austin et al., 1975). They made the key observation that at temperatures below about 160 K, rebinding of carbon monoxide after flash photolysis with a microsecond laser is highly nonexponential and appears to be a single process extending from microseconds to kiloseconds. The extended rebinding was interpreted as arising from a continuous distribution of exponential processes. This observation of a continuous distribution led to the postulate of conformational substates, in which myoglobin exists in a continuum of slightly different conformations, each with a different geminate-rebinding rate. At low temperatures, these conformations appear to be "frozen", that is, they interconvert much more slowly than ligand rebinding. As the temperature is increased above the glass transition temperature of the glycerol/water solvent, geminate ligand rebinding becomes multiphasic and, in fact, appears to slow down. Further increase in temperature permits the photodissociated ligand to escape into the solvent, thus decreasing the amount of geminate rebinding. At room temperature, all ligands escape into the solvent during the 1-μs photolysis pulse, and the geminate yield vanishes; ligand rebinding from the solvent takes place in a simple bimolecular process. The interconversion of conformational substates is fast compared to the time scale of the bimolecular process, and a single process (which is exponential under pseudo-first-order conditions) is observed with a conformationally averaged rate.

All of these observations could be accounted for within the framework of a simple reversible *sequential* model with multiple geminate intermediates (Austin et al., 1975; Beece et al., 1980):

$$A \rightleftarrows B \rightleftarrows C \rightleftarrows D \rightleftarrows S$$

In this model, the ligand is bound to the heme in state A, is in the region adjacent to the heme called the "heme pocket" in geminate state B, and is in the solvent in state S. States C and D represent two additional geminate intermediates that were required to describe the multiphasic geminate-ligand-rebinding kinetics in the temperature range from 200 to about 280 K. These additional intermediates were interpreted as arising from free-energy wells in other parts of the protein or in the hydration shell. In this scheme, the path of the ligand leaving and entering the protein is one in which it must overcome a series of barriers. This picture is consistent with the early X-ray finding that there is no open path between the solvent and the heme (Nobbs, 1966; Perutz & Matthews, 1966), and ligand binding must take place via a displacement of amino acid side chains, providing a structural explanation for at least one geminate state. According to this model, only state B is populated by photodissociation below 160 K. As the temperature is increased, the thermal energy becomes sufficient to overcome the barrier between B and C, as well as the subsequent barriers, so that geminate ligand rebinding becomes multiphasic, with ligands returning to the heme after overcoming one, two, or three barriers, and the overall rate of geminate rebinding appears to decrease. This sequential model was further elaborated by Frauenfelder and co-workers (Beece et al., 1980) to fit the complete time course of the rebinding kinetics after about 1 μs as a function of solvent viscosity between 200 and 330 K and for viscosities ranging from about 10 to $>10^5$ cP. The data were modeled using a modified Kramers rate expression (Kramers, 1940), by assuming that the rate is inversely proportional to a fractional power of the viscosity and reaches a limiting value at infinite viscosity. This analysis yielded viscosity-dependent rates for all of the steps with the exception of the ligand-binding step, which was assumed to be viscosity independent.

It appeared, then, that the sequential model was capable of providing a satisfactory explanation of the complete time course of myoglobin ligand binding over a wide range of temperatures and viscosities. It also successfully explained geminate-rebinding kinetics at ambient temperatures in hemoglobin (Hofrichter et al., 1983). There is, however, a fundamental problem with the sequential model in that it does not explicitly address the question of the effect of conformational relaxation of the protein on the kinetics. In the sequential model, the interconversion among conformational substates was only treated in the limits of frozen states, i.e., no interconversion, below 180 K, and complete averaging, i.e., interconversion rates that are instantaneous relative to geminate rebinding, above about 200 K. Furthermore, time-resolved studies on hemoglobin had shown that conformational relaxation did indeed occur on the same time scale as geminate rebinding at room temperature (Lyons & Friedman, 1980; Hofrichter et al., 1983). Moreover, the geminate kinetics of carbon monoxide rebinding to myoglobin in aqueous solutions at room temperature were found to differ considerably from those predicted by extrapolating the low-temperature data (Henry et al., 1983a), suggesting that some conformational change occurred above the glass transition temperature of the solvent. It was proposed that this conformational relaxation could alter the geminate-rebinding rate, suggesting a more complex model at room temperature (Henry et al., 1983b; Hofrichter et al., 1985; Friedman, 1985).

The first formal model to deal explicitly with simultaneous geminate rebinding and protein relaxation was developed by Agmon and Hopfield (1983). They modeled the protein conformational relaxation as one-dimensional diffusion along a single, generalized protein coordinate and the ligand rebinding as taking place along an independent reaction coordinate with the barrier height dependent upon the position of the protein coordinate. With this model, which only dealt with the geminate-rebinding step, they were able to generate multiphasic geminate rebinding without having to invoke additional barriers to ligand motion as in the sequential model. Another important feature of this model is that it could qualitatively explain the apparent slowing of geminate rebinding as the temperature was increased above the solvent glass transition as arising from a relaxation from a fast rebinding distribution of conformational substates associated

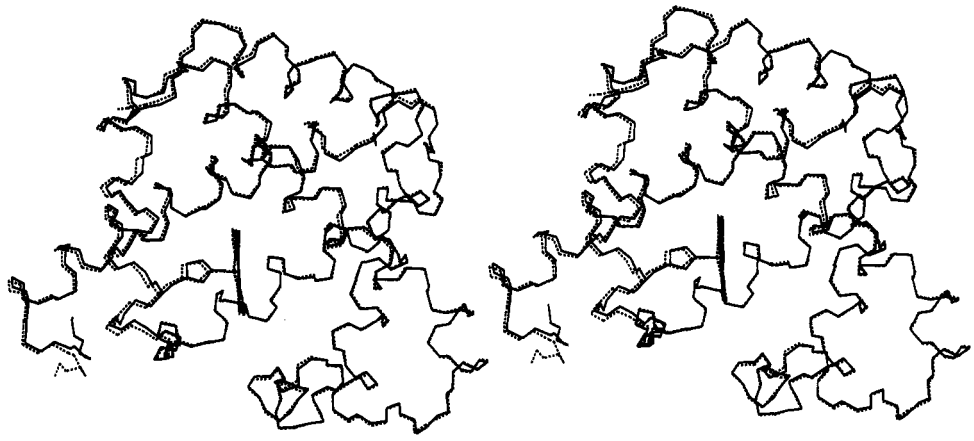

FIGURE 1: Comparison of the structures of deoxymyoglobin and its complex with carbon monoxide. Only the bonds connecting the polypeptide backbone atoms are shown in addition to the heme and axial ligands. The dashed lines are the structure of deoxymyoglobin (Phillips, Brookhaven Data Bank File 1MBD), while the continuous lines are the structure of the carbon monoxide complex (Kuriyan et al., Brookhaven Data Bank File 1MBC). The two structures are superimposed by a least-squares procedure using only the backbone atoms from the B, C, and G helices. This is the superposition used by Kuriyan et al. (1986). The shift of the protein atoms away from the heme on the side of the bound histidine is barely perceptible.

with the liganded molecule to a slow rebinding distribution of conformational substates associated with the unliganded molecule.

More recently, Frauenfelder and colleagues (Steinbach et al., 1991) have applied the Agmon–Hopfield approach to reanalyzing the ligand-binding kinetics. By analogy with the relaxation of glasses, they used a stretched exponential of the form $\exp(-kt)^{\beta}$ to describe the *assumed* protein relaxation, called Mb* to Mb, which resulted in an increase in the barrier for rebinding above about 180 K. There are two possible shortcomings of the model of Steinbach et al. (1991). First, the kinetics of the conformational relaxation of the protein were not measured. Second, their model does not include the possibility of rebinding from more than one geminate state as described earlier (Austin et al., 1975; Beece et al., 1980).

From the above discussion, it should be clear that the critical missing element in understanding the mechanism of ligand binding in myoglobin is the direct measurement and characterization of the kinetics of protein conformational relaxation. A comparison of the X-ray crystallographic structures of myoglobin and its carbon monoxide complex shows that the conformational changes between the liganded and unliganded molecules are quite small: there is a localized rearrangement of residues on the distal side of the heme resulting from removal of the ligand as well as a very small global motion of the protein atoms on the proximal side caused by displacement of the iron from the heme plane (Phillips, 1980; Hanson & Schoenborn, 1981; Kuriyan et al., 1986) (Figure 1). The average displacement away from the heme in this global motion is only about 0.02 nm. The spectral changes associated with these conformational changes are therefore expected to be very small compared to the spectral changes associated with ligand dissociation and rebinding. Nevertheless, the importance of the problem has sparked a considerable effort to measure the kinetics of conformational changes in myoglobin.

At temperatures less than 160 K, deoxyheme optical changes of the near-infrared band, originally attributed to conformational relaxation (Ansari et al., 1985), were subsequently shown to arise from "kinetic hole burning" (Campbell et al., 1987; Agmon, 1988; Nienhaus et al., 1992), that is, faster binding conformational substates possess a longer wavelength near-infrared band, resulting in an apparent shift of this band to shorter wavelengths as ligand binding proceeds. Kinetics of protein conformational changes in the religanded state have been measured by monitoring the infrared spectrum of the geminately recombined CO near the glass transition in glycerol/water solvents (Young et al., 1991). Until recently, measurements of protein relaxation at room temperature either have been unsuccessful or have produced extremely limited data. After the initial report from this laboratory that there were no spectral changes of the deoxyheme photoproduct after about 30 ns in aqueous solutions (Henry et al., 1983a), most of the effort was directed toward experiments in the subnanosecond time regime. Subnanosecond conformational changes were inferred from differences in resonance Raman frequencies of porphyrin modes at 30 ps and 10 ns (Dasgupta et al., 1985), but no time course was measured. Other Raman and optical studies showed no differences at these time delays, presumably due to a lack of sensitivity of the measurements (Findsen et al., 1985; Janes et al., 1988). A sub-30-ps conformational change has, however, been suggested from transient grating experiments (Genberg et al., 1991; Richard et al., 1992). There have also been limited kinetic observations of a protein conformational change with a relaxation time of 100–200 ps in the deoxy photoproduct from circular dichroism measurements (Xie & Simon, 1991).

Our approach to determining conformational relaxation kinetics in myoglobin has been to measure precise optical absorption spectra of the heme in the Soret region following photodissociation with 10-ns pulses. In a previous study, we found that the Soret spectrum at 30 ns following photodissociation was slightly different from that of the immediate photoproduct in water at room temperature (Henry et al., 1983a). In the present study, we have been able to examine the kinetics of the deoxyheme spectral changes by using improved instrumentation and by performing the measurements in glycerol/water mixtures to increase the viscosity and thereby slow the kinetics into the time regime accessible to our nanosecond spectrometer. By systematically varying both the temperature and the viscosity, it has been possible to investigate the conformational relaxation kinetics in detail and to relate these kinetics to ligand binding by theoretical modeling. A brief account of part of this study has already appeared (Ansari et al., 1992). We should also point out that Lambright et al. (1991) and Tian et al. (1992) have independently observed the kinetics of these deoxymyoglobin spectral changes, but there was no investigation of the viscosity

dependence and no theoretical modeling. Since this work was completed, extensive data on subnanosecond protein relaxation kinetics has been reported by Anfinrud and coworkers (Lim et al., 1993; Jackson et al., 1994) who have made very precise measurements on the time dependence of the shift in the frequency of the near-infrared band. They observed a continuous change in this frequency from 2 ps to about 1 μs, which can be fit with a highly stretched exponential.

Although time-resolved spectroscopy is becoming a widespread technique, there is still no straightforward methodology for kinetic analysis of multiwavelength data. In the present work, novel numerical techniques are introduced for fitting multiwavelength kinetic data that should be generally useful for any type of time-resolved spectroscopy. More specifically, we represent the data in compact form for kinetic modeling using singular value decomposition and use a matrix transformation procedure that allows us to separate the spectral changes due to ligand binding and protein conformational changes from the spectral changes due to solvent and temperature changes. To overcome the local minimum problem in data fitting, we use a simulated annealing approach with a Metropolis-type Monte Carlo algorithm.

MATERIALS AND METHODS

Sperm whale skeletal muscle metmyoglobin was purified as previously described (Henry et al., 1983a); "50%" (56% w/w) and "75%" (79% w/w) glycerol/water samples were obtained by mixing equal volumes of glycerol and aqueous protein solution or 3 volumes of glycerol to 1 volume of aqueous protein solution, respectively. The carbon monoxide (CO) complex was formed by reduction with sodium dithionite and equilibration with 1 atm of CO. The final samples contained 116–134 μM protein, 0.1 M potassium phosphate (pH 7.0), and 0.01 M sodium dithionite.

Time-resolved optical absorption spectra following photodissociation were measured with two Q-switched Nd:YAG lasers producing 10-ns (fwhm) pulses (Hofrichter et al., 1991, 1994). The 532-nm second harmonic of one laser was used to photolyze the sample, while the spontaneous emission of a dye (stilbene 420) excited by the 355-nm third harmonic of the second laser was used as a probe. A $^1/_4$-m spectrograph and silicon vidicon tube read by an OMA detector controller (PAR 1216) were used for measuring time-resolved absorption spectra. To evaluate and eliminate the effects of photoselection, complete sets of spectra were measured using both parallel and perpendicular orientations of the linearly polarized excitation and probe pulses (Ansari et al., 1993). For each set of solvent conditions, temperature, and polarization, an experiment consisted of approximately 100 spectra measured at logarithmically spaced time intervals from 20 ns to about 90 ms after photolysis together with linearly spaced data over the time interval from about −20 to 20 ns. The degree of photolysis in most experiments was about 95%. The data could, however, be accurately scaled to 100% photolysis using the measured anisotropy, the photoselection theory for polarized photolysis experiments of Ansari and Szabo (1993), and the observed order parameter for the internal heme dynamics of 0.95 (Ansari et al., 1993).

Data Reduction. Each set of time-resolved spectra was first analyzed using singular value decomposition (SVD) which transforms the data matrix **A** into a product of three matrices, i.e., $\mathbf{A} = \mathbf{USV}^T$ (Henry & Hofrichter, 1992). The columns of **U** are a set of orthonormal basis spectra that describe all the spectra in the data matrix **A**; the columns of **V** are the corresponding amplitudes as a function of time and conditions; and **S** is a diagonal matrix with non-negative elements called the singular values which are a measure of the contribution of the corresponding basis spectrum to the data matrix. SVD has the useful property that the components with the k largest singular values provide the best (in the least-squares sense) k–component fit to the data. At each solvent composition and temperature, the transient spectra could be described to very good accuracy by two basis spectra; the first was an "average" deoxyMb–MbCO difference spectrum, and the second was primarily a derivative around the deoxy peak.

In order to compare and quantitatively analyze the data collected under different conditions of temperature and viscosity, a "global" data matrix was constructed from the first 12 SVD components from the individual experiments in the three solvents (0%, 50%, and 75% glycerol). The SVD of this global matrix provides a convenient and compact representation of all of the data in which the time-dependent amplitudes for all sets of conditions refer to the same set of basis spectra. The largest contribution to noise in these measurements arose from base-line offsets which result from fluctuations in the intensity of the probe laser. These offsets are uncorrelated with delay time and were removed as described by Jones et al. (1992). Isotropic spectra were calculated from the subset of the resulting **V** matrix which corresponded to the parallel and perpendicular absorbances measured under each set of conditions using the relation: $\Delta OD_{iso} = {}^1/_3(\Delta OD_{\parallel} + 2\Delta OD_{\perp})$. Prior to the isotropic averaging, the differences in the amplitudes of the spectra due to variations in the level of photolysis between the parallel and perpendicular data sets were eliminated by matching the amplitudes at times long compared to the rotational correlation time of the molecule. The SVD analysis showed that a simultaneous description of all of the data required four basis spectra.

When the data were represented in terms of a single set of basis spectra, systematic dependencies of the difference spectra on temperature and solvent composition became readily apparent. An important property of the SVD carried out on data collected at a single set of conditions is that the number of basis spectra required to describe the data (plus one, since we are measuring difference spectra) provides a lower limit on the number of absorbing species present in the system (Henry & Hofrichter, 1992). The spectra of heme proteins are known to be temperature and solvent dependent (Schomacker & Champion, 1986; Cordone et al., 1986, 1988; Leone et al., 1987), so these spectral changes are superimposed on those produced by the kinetic intermediates when temperature and/or solution conditions are altered. It therefore becomes important to determine whether the additional spectral components obtained from the SVD of the global data set result from additional intermediate states or from condition-dependent differences in the absorption spectra of a smaller number of distinct molecular species. To address this problem, we asked whether the temperature- and composition-dependent effects in the measured difference spectra could be separated from those which resulted from time-dependent changes in the spectra. We assumed that, at least to a first approximation, the effects of solvent and temperature on the spectra of all deoxy photoproduct species could be treated as identical. We then asked if an orthogonal transformation of U_2, U_3, and U_4 which optimized our ability to represent V_3 and V_4 in terms of V_1 under each set of conditions x would provide an accurate description of the observed amplitudes of these two components. If such a transformation is found, it describes the temperature and

solvent dependences of the *average* deoxy–CO difference spectrum under each set of conditions as a linear combination of U_1, U_3, and U_4, using only a single set of time-dependent amplitudes, that is, the values of V_1 obtained under conditions x.

To carry out the search for this transformation, we defined a rotation matrix, $\mathbf{R}(\theta,\phi,\zeta)$, where θ, ϕ, and ζ are Euler angles. We wish to determine the Euler angles which minimize the residuals (δ^2) between the third and fourth components of the rotated V matrix, $\mathbf{V^R} = \mathbf{RV}$, associated with a single set of conditions and their representation as a scale factor times the corresponding V_1:

$$\delta^2 = \sum_x \sum_{j=3,4} \sum_{i \in x} (V^R_{ij} - g_{jx} V_{i1})^2 \qquad (1)$$

The notation $\{x\}$ in eq 1 denotes some set of conditions which define a single experiment (that is, a subset of values for the rows index of the global V), and g_{jx} denotes the linear least-squares solution to the equation $V^R_{ij}(i \in x) = g_{jx} V_{i1}(i \in x)$. The optimal transformation permitted more than 95% of the original amplitude of both the third and fourth SVD components to be represented as having the same time dependence as the corresponding V_1. The residuals produced by representing V_3 and V_4 in terms of V_1 were much smaller than those which were discarded in truncating the SVD to four components.

This transformation allows us to represent the time dependence of the measured spectra under all temperature and solvent conditions in terms of two basis spectra. To model the kinetics of the system, we therefore only need to consider the time dependence of the first two components. One of these basis spectra is the second column of U, the time dependence of which is described by the second column of V. The time-dependent amplitudes of the other basis spectrum are described by the first column of V; the basis spectrum associated with V_1 describes the average deoxy–CO difference spectrum under each set of conditions and is a prescribed linear combination of U_1, U_3, and U_4. It is important to emphasize that the coefficients g_{jx} in eq 1 are specified prior to carrying out the fit to the kinetic data and therefore are not included as parameters in the fitting procedure described below. Comparison of the data matrix reconstructed from this representation with the original data shows that the average magnitude of the difference between the two is less than 4×10^{-4} OD unit. The maximum magnitudes of the measured absorbance changes were approximately 0.5 OD, so the largest spectral changes are represented to an accuracy which is better than 99.9% by this representation of the data.

Kinetic Modeling. To quantitatively relate the experimental results to kinetic models, we need to describe the V components, obtained from the SVD analysis described above, as linear combinations of the populations of the species in the model. At each temperature and viscosity, the amplitudes of the first two components are linear combinations of the concentrations of the molecular species which define the model:

$$V_j(t,T,\eta) = q_j(T,\eta) \sum_m p_{jm} c_m(t,T,\eta) \qquad j = 1, 2 \qquad (2)$$

where c_m is the concentration of the mth species, p_{jm} are the coefficients that describe the spectrum of the mth molecular species at some reference temperature T_0 and solvent conditions η_0, and $q_j(T,\eta)$ accounts for temperature- and solvent-dependent amplitude changes in the basis spectra U_j. To simplify the problem, we assume that the difference spectra between the deoxy species (represented by the second basis component) are identical at all temperatures and solvent conditions, i.e., $q_2(T,\eta) = 1$. This assumption is reasonable because the observed spectral changes are quite small and all of the deoxy photoproduct spectra arise from the same electronic transition of the heme, perturbed only by slight alterations in the protein conformation. The effects of solvent and temperature on the band shapes and peak positions for all of the deoxy spectra are, therefore, anticipated to be similar. The perturbations of the deoxyheme spectra by the solvent are also small and so are assumed to have, at most, a second-order effect on the magnitude of the spectral changes which result from the changes in the conformation of the unliganded protein. The molecular spectrum of the mth species at $T = T_0$ and $\eta = \eta_0$ may then be written in terms of the first two columns of U as

$$M_m(\lambda) = \sum_{j=1}^{2} q_j p_{jm} s_j U_j(\lambda) \qquad (3)$$

where s_j is the singular value of basis spectrum U_j and p_{jm} and q_j are parameters to be varied in a least-squares fit to the data. For a model which contains n spectrally distinct molecular species, eq 3 requires $2n$ coefficients which describe the spectra of these species in terms of two SVD components. If it is further assumed that U_2 describes only the deoxy spectral change and has no contribution from ligand rebinding, then V_1 becomes a precise measure of the number of deoxyhemes (i.e., ligand rebinding) and $p_{1m} = p_{11}$ for all m; the number of coefficients required to describe the spectra of n species therefore reduces to $n + 1$. To describe the spectra of these n species under all conditions, the parameters which must be specified are a value of $q_1(T,\eta)p_{11}$ for each set of conditions and np_{2m} coefficients which are independent of temperature and solvent composition.

The time evolution of the system composition is calculated from a kinetic model. To obtain rates at temperatures and viscosities which differ from T_0 and η_0, we express the temperature and viscosity dependencies of the rate constants for each elementary step in the mechanism by an Arrhenius relation with a viscosity-dependent prefactor (Ansari et al., 1992):

$$k(T,\eta) = k(T_0,\eta_0)\frac{\sigma + \eta_0}{\sigma + \eta} \exp\left(\frac{E_0}{R}\left(\frac{1}{T_0} - \frac{1}{T}\right)\right) \qquad (4)$$

where η is the solvent viscosity and E_0 the activation energy. The parameter σ has units of viscosity and can be thought of as the contribution of the protein friction to the total friction (see below) (Ansari et al., 1992). The rate constants under all sets of conditions are parametrized in terms of $k(T_0, \eta_0)$, σ, and E_0. In the remainder of the paper, we shall refer to $k(T_0, \eta_0)$ as simply k. Since viscosity is a purely dynamical variable and therefore should have no effect on the equilibrium constants, the rates were further constrained by equating the value of σ for the forward and reverse rates.

For the bimolecular step that describes the entry of the ligand into the protein, we make an assumption motivated by the study of McKinnie and Olson (1981) which separates the effects of changing the solvent on the viscosity from the effects of changing the solvent on the chemical potential of the free CO. That is, we assume that the change in solvent has no effect on the difference between the free energies of the transition state and the free myoglobin, so that all of the change in the free energy of activation results from a change in the chemical potential of the free CO. This change in chemical

potential can be measured from the change in CO solubility (the solubilities are sufficiently low that activity coefficients can be ignored). We therefore scale the bimolecular rate constant by the ratio of the CO solubility under the conditions of the measurement to that of the reference conditions (20 °C, 0% glycerol) to obtain a rate constant that depends only on viscosity and temperature and not on the composition of the solvent. The solubility of CO ([CO_S]) at 20 °C has been measured for glycerol/water mixtures of varying composition (Ackerman & Berger, 1963; McKinnie & Olson, 1981); we use the numbers published by Mckinnie and Olson at 20 °C and model the temperature dependence of the solubilities in each of the solvents in terms of an enthalpy difference (E_s) between the CO in the gas phase and in the solvent:

$$[CO_S(T)] = [CO_S(293\ K)] \exp\left(\frac{E_S}{R}\left(\frac{1}{T} - \frac{1}{293\ K}\right)\right) \quad (5)$$

Both the temperature dependence of the CO solubility in each of the solvents and the temperature dependence of the activated entry step contribute to the temperature and solvent dependencies of the bimolecular step.

Fitting Procedure. The many-dimensional parameter space that describes a model at all temperatures and solvent conditions in terms of rate parameters, k, σ, and E_0 for each elementary step was explored in some detail. The residuals between the V components at each temperature and solvent condition and those predicted from a model were minimized in two stages. In the first stage, the residuals from the data in 75% glycerol at three temperatures (0, 15, and 30 °C) were minimized using a simulated annealing procedure (Kirkpatrick et al., 1983; Press et al., 1986) based on that introduced by Metropolis et al. (1953). Finding the point in parameter space which produces a global minimum in the value of χ^2 is analogous to the problem of finding the lowest free-energy state in a complex system. If the system is cooled rapidly to a low temperature, analogous to the case where a minimizer is started from a random point having a large χ^2, then the system can relax only to local minima, and the state which the system reaches is highly dependent on both the point from which it started and the rate of cooling. Finding a global minimum becomes more probable if the system is annealed, that is, if the potential surface is first explored at high temperature where a large number of states are accessible and the system is cooled slowly. Simulated annealing thus permits the system to get out of local minima in favor of finding better, more global, ones. The temperature can then be lowered gradually to permit the portions of this surface, which are characterized by smaller values of χ^2, to be explored in finer detail. This procedure serves two purposes: (i) it permits a coarse-grained and relatively efficient exploration of the features of the parameter space which are consistent with a relatively small subset of data and (ii) it permits a pathway from relatively random starting values to a set of parameters from which a more complete fit to all of the data can be carried out with a probability for success which is high enough to be productive without having to "tweak" the initial values by hand. In addition, the number of distinguishable parameter sets found provides valuable information on the number of minima in the accessible parameter space.

To minimize the number of parameters in this search, changes in solution viscosity which resulted from changes in sample temperature were not considered explicitly at this stage of the analysis; any contribution from the temperature dependence of the viscosity was included in the apparent activation energy for each rate. The rates were represented by a simple Arrhenius expression:

$$k(T) = k(T_0) \exp\left(\frac{E_a}{R}\left(\frac{1}{T_0} - \frac{1}{T}\right)\right) \quad (6)$$

The problem is to obtain sets of values for the rates k and activation energies E_a which provide a reasonably good representation of this data, starting from random values selected from a plausible set of starting values. Sets of trials were carried out over a range of decreasing values for a parameter which we denote as χ_o^2. χ_o^2 is a reference value for the standard error of the fit that is analogous to kT in a Boltzmann probability. The value of χ_o^2 was initially chosen to be large (1024) and then gradually decreased by factors of $2^{1/2}$. A random step in parameter space was always accepted if χ^2 decreased and accepted with a probability $\exp(-\delta\chi^2/\chi_o^2)$ if χ^2 increased. This χ_o^2-dependent probability allows the system to escape local minima: the probability of taking a large uphill step gets smaller as χ_o^2 is lowered. After a number of steps at one χ_o^2, large enough to allow the system to "equilibrate", χ_o^2 was decreased and the algorithm repeated. The sizes of the steps in parameter space taken at each value of χ_o^2 were empirically chosen so that approximately half of the steps were accepted. The initial values of the parameters at each χ_o^2 after the first were chosen as those that gave the smallest residuals at the previous value. After 15 annealing steps, or when the residuals did not go below χ_o^2, the parameters which produced the minimum value of χ^2 were stored for use as starting values for further minimization, as described below. The entire procedure was repeated multiple times from different sets of randomly chosen initial parameters.

Each set of minimized parameters obtained by this procedure was then used as starting values for minimization using a Marquardt–Levenberg algorithm (Marquardt, 1963). In these fits, the data for all temperatures and solvent conditions were fit simultaneously using the complete viscosity- and temperature-dependent descriptions of the rates (eq 4). In all of the fits χ^2 is defined as the sum of squared residuals between the data and the fit to the data, divided by the residuals obtained by subtracting two independent data sets measured under identical conditions.

The entire kinetic model analysis, including solution of the systems of differential equations describing the model, the simulated annealing, and the least-squares fitting with variable model parameters, was performed using a single computer program written by E. R. Henry (unpublished work). This program provides a versatile programming language interface to many matrix analysis, optimization, and other numerical procedures required for the analysis of experimental data. The procedures incorporated into this program for the solution of systems of ordinary differential equations were the LSODA routines from the public domain ODEPACK package; these routines incorporate methods for solution of stiff and nonstiff systems of equationsas well as automatic selection of the appropriate method (Hindmarsh, 1983; Petzold, 1983).

RESULTS AND DISCUSSION

The principal focus of this work has been to measure the kinetics of conformational relaxation in myoglobin following carbon monoxide photodissociation and to determine how this relaxation influences the kinetics of ligand binding. As pointed out in the introduction, conformational relaxation following photodissociation has been invoked in theoretical analyses of ligand-binding kinetics by Agmon and Hopfield (1983) and

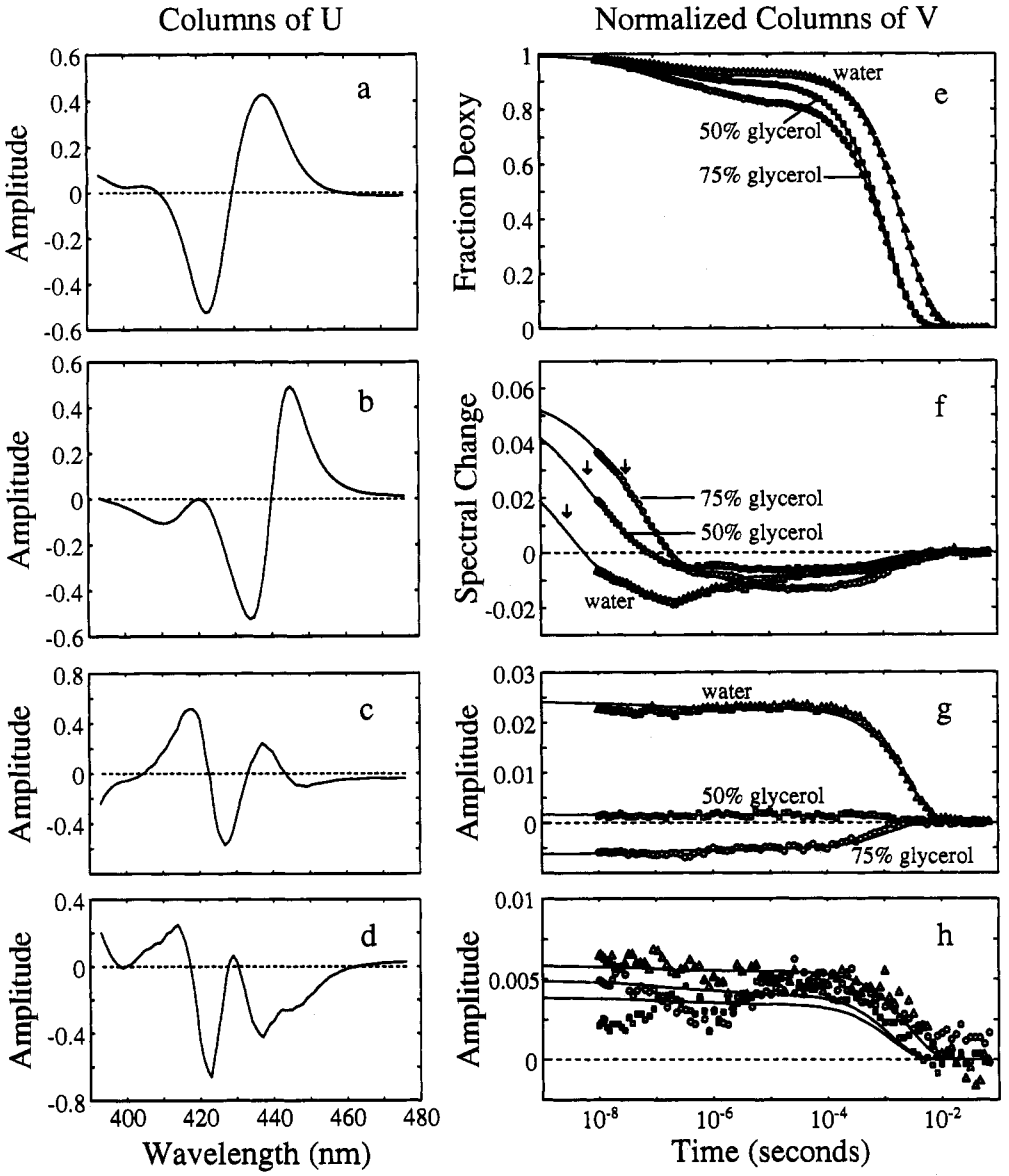

FIGURE 2: Singular value decomposition of the time-resolved absorption spectra following photodissociation of MbCO. The data under all sets of conditions (water at 5, 20, and 35 °C; 50% glycerol/water from −5 to 35 °C in steps of 5 °C; 75% glycerol/water from −5 to 35 °C in steps of 5 °C) were analyzed simultaneously. The first four components of the processed SVD of the data are shown. (a–d) Basis spectra (columns of U). Components 2–4 have been rotated in order to separate the temperature and solvent dependencies of the spectra into the 3rd and 4th components by optimizing the fit of their time-dependent amplitudes to the first column of V for the same set of conditions (see Materials and Methods). (e–g) Time-dependent amplitudes (columns of VS) at 20 °C. The data in three solvents are presented, (△) aqueous buffer, pH 7.0, (□) 50% glycerol/water, pH 7.0, and (○) 75% glycerol/water, pH 7.0. The *V* components are normalized such that the first component represents the fraction of deoxyhemes. (—) Phenomenological fits to the data obtained using eq 14 ($\chi^2 = 4.8$). The fits plotted in (g) and (h) have the same time-dependent amplitudes as the fits in (e) but have been scaled by a least-squares fit of the predicted time course to the data.

Frauenfelder and co-workers (Steinbach et al., 1991) but has not been directly observed until the present work (Ansari et al., 1992) and the recent studies by Lambright et al. (1991), Tian et al. (1992), Lim et al. (1993), and Jackson et al. (1994). In our experiments, high-precision transient absorption measurements in the Soret region have revealed spectral changes of the deoxyheme which are simultaneous with geminate ligand rebinding (Figure 2). We interpret the time course of these spectral changes as monitoring the kinetics of protein conformational changes. Increasing the viscosity markedly slows the rate of the initial conformational change, increases the amount of geminate rebinding, and extends geminate rebinding to longer times.

Since the protein conformational relaxation is strongly influenced by the solvent viscosity, we first discuss the problem of parametrizing the effects of solvent viscosity on rate constants. We then present an empirical characterization of the data. This is followed by an interpretation of the results in terms of a minimal kinetic model that incorporates the principal facts about myoglobin kinetics from the present studies as well as from previous work.

Effect of Viscosity on Rate Constants. Frictional effects on rate constants of chemical reactions have conventionally been discussed in terms of Kramer's theory (Kramers, 1940; Hänggi et al., 1990). Kramers idealized a chemical reaction as the one-dimensional motion of a particle from a potential well over a barrier under the influence of interactions with the solvent. His expression for the rate constant for this process is

$$k = \frac{\omega_0 \zeta}{4\pi\omega' m}\left(\sqrt{1+\left(\frac{2\omega' m}{\zeta}\right)^2} - 1\right)\exp(-E_0/RT) \quad (7)$$

where ω_0 is the frequency of the well, ζ is the friction constant, m is the mass of the particle, ω' is the frequency of the inverted barrier, and E_0 is the barrier height. In the limit of high friction, where $2\omega' m \ll \zeta$, eq 7 simplifies to

$$k = \frac{\omega_0 \omega' m}{2\pi\zeta} \exp(-E_0/RT) \tag{8}$$

which predicts that the rate is inversely proportional to the friction.

Equation 8 must be modified for proteins. Since only a fraction of the atoms of a protein molecule are in contact with solvent atoms, two sources of friction must be considered, the friction of the solvent which retards the motion of atoms on the surface of the protein and the internal friction of the protein which slows down the motion of protein atoms relative to each other (McCammon et al., 1979; Loncharich et al., 1992). Assuming that the frictional effects of the protein and solvent are additive, the Kramers expression for the rate constant becomes

$$k = \frac{B}{\alpha\zeta_p + (1-\alpha)\zeta_s} \exp(-E_0/RT) \tag{9}$$

where B is a viscosity- and temperature-independent prefactor that depends on the shape of the potential surface, ζ_p is the friction constant for motion in the protein, ζ_s is the friction constant for motion in the solvent which, according to Stokes' law ($\zeta = 6\pi\eta r$), is proportional to its viscosity, and α is a factor which weights the contribution of the two kinds of friction. The parameter α may be naively identified with the fraction of the protein atoms that are not in contact with solvent atoms. If we ignore the dependence of the protein friction constant on the solvent viscosity and temperature (as well as on the location within the protein), the preexponential factor can be written in terms of the known solvent viscosity η and the adjustable parameters C and σ:

$$k(T,\eta) = \frac{C}{\sigma + \eta} \exp(-E_0/RT) \tag{10}$$

which is equivalent to eq 4. In a slightly different empirical analysis of the initial conformational relaxation, Ansari et al. (1992) found that the dependence of the rate on viscosity exhibits the form predicted by eq 10, with a rate approaching viscosity independence at low viscosities ($\eta < \sigma$) and an inverse first-power viscosity dependence at high viscosities ($\eta \gg \sigma$).

In a previous analysis of ligand-binding data, using the sequential model discussed in the introduction, Beece et al. (1980) parametrized the rate constants for ligand motion using a relation of the form:

$$k(T,\eta) = \left(A^0 + \frac{A}{\eta^\kappa}\right) \exp(-E_0/RT) \tag{11}$$

where the exponent κ was restricted to values between 0 and 1 to account for the attenuation of the effect of solvent viscosity by the protein (Gavish, 1980, 1986). The use of eq 11 was motivated by the fact that the observed rates appeared to reach a saturating value at very high viscosities ($>10^4$ cP) and to have a fractional viscosity dependence at intermediate viscosities (10–10^4 cP). As pointed out in the introduction, there is no explicit treatment of conformational relaxation in a sequential model. The rates derived by Beece et al. (1980) are therefore only apparent rates and may contain contributions from conformational relaxation as well as ligand motion.

In general, we might expect two qualitatively different classes of dynamical processes in proteins. In the first, which is typified by a conformational change of the protein that requires displacement of solvent atoms, motion along the reaction coordinate is damped because of direct interaction between the solvent and the protein atoms. Kramers' equation, modified as in eq 10 to include contributions from protein friction, is applicable for this process. In the second kind of process, which is typified by the motion of ligands inside the protein or the catalytic step of an enzyme, the specific molecular coordinates which are changed and thereby define the reaction coordinate are not directly coupled to the solvent; the solvent viscosity only affects the dynamics of the process *indirectly* through its influence on the conformational dynamics of the protein. The viscosity dependence for this process shows deviations from the Kramers' behavior (Agmon & Hopfield, 1983; Agmon & Kosloff, 1987). Zwanzig (1992) has recently pointed out an interesting situation in which ligand motion through a bottleneck has no viscosity dependence per se but an apparent fractional viscosity dependence can arise if the radius of the bottleneck fluctuates on the same time scale as the ligand motion and if the rate of decay of the fluctuation, which may be identified with protein motions, is inversely proportional to the solvent viscosity. Therefore, for the second kind of process, a fractional viscosity dependence may be a better description in the high-viscosity limit. In our kinetic modeling, we shall treat conformational relaxations and ligand motion explicitly and, for simplicity, use eq 10 to describe both types of rate processes. In our admittedly highly simplified parametrization, we may use the magnitude of the parameter σ, which is proportional to $\zeta_p\alpha/(1-\alpha)$, to tell us something about the nature of the structural change associated with the motion along the reaction coordinate. For example, a localized conformational change in the interior of the protein, with α close to 1, would yield a large value for σ, whereas a global conformational change would result in a small value for σ.

Finally, we should point out the connection between our expression for the rate constant and the equation used by Steinbach et al. (1991) for the protein relaxation that was assumed in fitting their ligand-rebinding data, i.e.,

$$\kappa(T) = A \exp[-(E/RT)^2] \tag{12}$$

If we substitute the relation for the viscosity $\eta = \eta_\infty \exp[(T_0/T)^2]$ (Bässler, 1987), which provides an excellent fit to the viscosity data over a wide range of viscosity, then eq 10 becomes, for $\eta \gg \sigma$:

$$k(T,\eta) = \frac{C}{\eta_\infty} \exp[-(T_0/T)^2 - (E_0/RT)] \tag{13}$$

Iben et al. (1989) have found that T_0 for 75% glycerol/water is about 1130 K, indicating that if E_0 is of the order of 2 kcal/mol or less, the first term will dominate at the temperatures of the measurements of Steinbach et al. (1991) and eqs 12 and 13 become isomorphic with $E = RT_0$.

Description of the Kinetic Data. Transient absorption spectra of Mb after photodissociation of the bound ligand were measured for two different glycerol concentrations (50% and 75% glycerol/water) in the temperature range –5 to 35 °C and in water in the temperature range 5 to 35 °C. The spectra under all conditions were analyzed using the SVD procedure described in Materials and Methods. Pairs of V components under each set of conditions, corresponding to experiments with the probe beam oriented both parallel and

perpendicular to the excitation beam, were isotropically averaged to eliminate changes in the absorption spectra resulting from rotational diffusion of the photoselected population which occurs on the same time scale as geminate rebinding (Jones et al., 1992; Ansari & Szabo, 1993; Ansari et al., 1993; Hofrichter et al., 1994). The spectral information at all times and under all conditions is well described in terms of four basis spectra with condition-dependent amplitudes. Further analysis of these four basis spectra (see Materials and Methods) showed that the data can be represented in terms of two spectral components having linearly independent amplitudes under each set of conditions and two additional components that describe temperature- and solvent-dependent differences in the time-averaged deoxy–CO difference spectra. The higher order components, which comprise less than 0.1% of the maximum data amplitudes, have been neglected.

Figure 2 shows the four spectral components and their amplitudes at 20 °C for the three different solvents. The first component is a deoxy–CO difference spectrum averaged over all times and all sets of conditions; the time-dependent amplitudes of this component for each set of conditions are proportional to the fraction of deoxyhemes in the sample and represent a very good approximation to the kinetics of ligand rebinding. The higher order SVD components represent deviations from this average spectrum. The second basis spectrum (U_2) is, to a good approximation, a derivative spectrum about the deoxyMb peak, and this component describes all of the observed deoxy spectral changes; the corresponding amplitudes are determined by both the kinetics of ligand rebinding and the kinetics of conformational changes of the deoxy species. The presence of this component, together with the fact that its amplitudes are linearly independent from those of U_1, implies that there are at least two spectrally distinct photoproduct species in the system with distinguishable time-dependent populations. As described in detail in Materials and Methods, the third and fourth components were found to represent temperature- and solvent-dependent differences in the average deoxy–CO difference spectra. (These components are absent in the SVD of an individual data set.) For each temperature and solvent composition, the time-dependent amplitudes of these components are proportional to the amplitude of the first component. The results of this analysis show that the *kinetic* information under each set of conditions can be represented in terms of only *two* basis spectra, and their associated amplitudes provide an optimized description of ligand rebinding (V_1) and the change in the deoxyheme spectra (V_2).

The most striking feature of the time-dependent amplitudes in Figure 2 is that the amplitude of the deoxy spectral changes observed at times less than about 300 ns increases dramatically as the viscosity increases at 20 °C (Figure 2f). When the temperature is lowered under fixed solvent conditions, a similar increase in this amplitude is observed. The first two columns of V measured in 75% glycerol/water at temperatures from 0 to 30 °C are shown in Figure 3. The initial amplitude of V_2 increases by nearly a factor of 2 and the characteristic time for its initial decay increases by about a factor of 6 as the temperature decreases from 35 to −5 °C. These effects of temperature are comparable in magnitude to those observed when the viscosity is increased (Figure 2). The observed effects of experimental conditions on the amplitude of the deoxy spectral change are much too large to be ascribed to temperature- and solvent-dependent differences in the spectra of the deoxy photoproduct. If the temperature and solvent dependencies of these spectra are assumed to be comparable

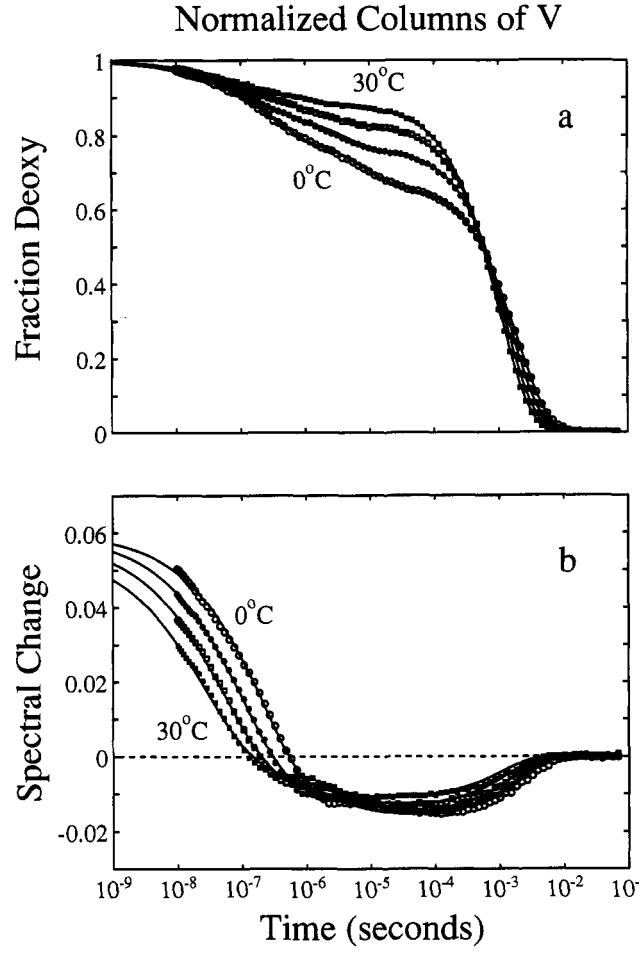

FIGURE 3: Temperature dependence of the kinetics of ligand rebinding and spectral changes. The time-dependent amplitudes corresponding to (a) the first component and (b) the second component are plotted as a function of time. The data plotted are for 75% glycerol/water at four temperatures: (○) 0 °C, (●) 10 °C, (□) 20 °C, and (■) 30 °C and have been normalized as in Figure 2. (—) Phenomonological fits to the data obtained using eq 14 (χ^2 = 4.8).

to those observed for the equilibrium deoxy spectrum by Cordone and co-workers (Cordone et al., 1986, 1988; Leone et al., 1987), the amplitudes are predicted to change by only 4–5% over this range of temperature and solvent conditions. While the possibility that the actual differences in conformation between MbCO and deoxyMb are solvent and temperature dependent cannot be ruled out, the most reasonable explanation for the increase in the observed amplitudes is that the rates decrease as the temperature is lowered or the solvent viscosity raised. As a result, more of the process responsible for the amplitude change becomes observable at times longer than our laser pulsewidth.

It is instructive to explore some of the features of the data using a model-independent analysis. The parametrization of this empirical description must be assumed a priori to permit an efficient and compact description of the data. In particular, the parametrization selected must account for the changes in the amplitude of the deoxy spectral change observed in Figures 2 and 3. We assume that the changes observed arise from differences in the rate of conformational relaxation and not from solvent- and temperature-dependent changes in the photoproduct spectra. The V components that describe the kinetics of ligand rebinding and deoxy spectral changes in the temperature range −5 to 35 °C were represented by three unimolecular processes (in the geminate phase) and one bimolecular process in which ligands rebind from the solvent:

$$V_j(t,T,\eta) = \sum_{l=1}^{3} \alpha_{jl}(T,\eta) \exp[-(k_l t)^{\beta_l}] + \alpha_{j4}(T,\eta) \frac{[CO] - [Mb]}{[CO] \exp[k_4 t([CO] - [Mb])] - [Mb]} \quad (14)$$

[Mb] is the protein concentration that contributes to the bimolecular process and, for 100% photolysis, is given by $\alpha_{14}/\sum\alpha_{1l}$ times the total protein concentration; [CO] is the free CO plus the CO liganded to Mb which escapes into the solvent after photolysis. We assumed that α_{21}, the amplitude of the spectral change which takes place between the initial photoproduct and the state observed at the end of the first conformational relaxation, is independent of both temperature and solvent conditions. The value of β_1 was allowed to vary, but the second and third processes were assumed to be exponential (i.e., $\beta_2 = 1$; $\beta_3 = 1$). The use of a stretched exponential to describe the first relaxation was motivated primarily by the fact that the existing data at low temperature and/or high solvent viscosities for times longer than about 10 ns strongly suggest that this process is not adequately described by a single exponential relaxation (Beece et al., 1980; Lambright et al., 1991; Ansari et al., 1992; Tian et al., 1992). The dependence of the rates for these processes on experimental conditions was described by eq 4. The reference conditions for $k(T_0,\eta_0)$ were chosen to be 5 °C in 75% glycerol/water.

The parameters that describe the rates for these relaxations and the corresponding amplitudes are summarized in Table 1, and the fit to a subset of the V components is shown in Figures 2 and 3. The optimal value of β_1, 0.59, supports our assumption that this process is more complex than a single exponential relaxation and therefore involves more than a single intermediate state (an alternative description of the kinetics of this relaxation which would also be consistent with the data would be as a sum of two exponentials having rates which differ by about a factor of 10 and roughly equal amplitudes). The dependence of the rates for the four relaxations on solvent viscosity is plotted in Figure 4. The first relaxation rate (k_1) exhibits a strong viscosity dependence ($\sigma = 4$). The rates for the second and third processes (k_2 and k_3) exhibit viscosity dependence above about 100 cP, and the rate which describes the bimolecular process (k_4) is nearly viscosity independent.

The amplitudes obtained from this analysis are presented in Figure 5. The amplitudes α_{1l} correspond to ligand-rebinding amplitudes in each relaxation l. The fact that the ligand-rebinding amplitudes for each of the geminate phases are significant (Figure 5a–c) shows that geminate ligand rebinding is distinctly nonexponential in all three solvents. The amplitudes α_{2l} corresponding to the deoxy spectral changes are more difficult to interpret since they reflect contributions from both ligand rebinding (the amplitudes of the deoxy spectral changes decrease as the ligands rebind) and from protein conformational changes. The amplitudes which result from the conformational changes alone are obtained as follows: the photoproduct spectrum prior to relaxation l, $PS_l(\lambda)$, may be written in terms of the amplitudes α_{jl} and the basis spectra U_j as

$$PS_l(\lambda) = \left(\sum_{j=1}^{2}\sum_{k=l}^{4} U_j(\lambda)\alpha_{jk}\right)\left(\frac{\sum_{k=1}^{4}\alpha_{1k}}{\sum_{k=l}^{4}\alpha_{1k}}\right) \quad (15)$$

Table 1: Summary of Parameters Used in the Empirical Description

rate parameters	process 1[a]	process 2	process 3	process 4
$k(T,\eta)$ (s^{-1})[b]	3.2×10^7	6.5×10^6	4.1×10^5	1.7×10^6 M^{-1}
σ (cP)	4.7	114	69	1×10^3
E_0 (kcal/mol)	≈0	3.1	3.7	2.4

solvent	T (°C)	α_{11}[c]	α_{12}	α_{22}	α_{13}	α_{23}	α_{14}	α_{24}
75% gly	−5	0.170	0.083	0.021	0.135	0.004	0.611	−0.018
	0	0.132	0.077	0.020	0.122	0.005	0.669	−0.016
	5	0.102	0.071	0.019	0.107	0.007	0.720	−0.016
	10	0.079	0.067	0.018	0.088	0.007	0.766	−0.015
	15	0.061	0.062	0.016	0.077	0.007	0.800	−0.015
	20	0.048	0.058	0.014	0.063	0.007	0.831	−0.013
	25	0.038	0.054	0.012	0.052	0.007	0.855	−0.012
	30	0.030	0.051	0.009	0.039	0.007	0.879	−0.011
	35	0.024	0.048	0.006	0.026	0.007	0.902	−0.011
50% gly	−5	0.039	0.064	0.028	0.116	−0.002	0.781	−0.011
	0	0.034	0.059	0.025	0.094	−0.002	0.813	−0.009
	5	0.030	0.055	0.021	0.075	−0.002	0.839	−0.009
	10	0.027	0.052	0.018	0.060	−0.001	0.862	−0.007
	15	0.024	0.049	0.014	0.046	0.0	0.881	−0.007
	20	0.021	0.046	0.011	0.035	0.001	0.898	−0.006
	25	0.019	0.043	0.008	0.028	0.002	0.910	−0.005
	30	0.018	0.041	0.005	0.020	0.002	0.922	−0.005
	35	0.016	0.039	0.003	0.013	0.003	0.932	−0.005
water	5	0.018	0.040	0.016	0.040	−0.015	0.903	−0.008
	20	0.018	0.033	0.009	0.009	−0.011	0.941	−0.009
	35	0.018	0.028	0.002	0.001	−0.008	0.953	−0.006

[a] Process 1 is a stretched exponential with $\beta_1 = 0.59$. [b] The rates are calculated at $T = 20$ °C and $\eta = 56.6$ cP, the viscosity of 75% glycerol/water solution. [c] The amplitudes are normalized so that $\sum\alpha_{1k} = 1$; α_{21} (0.05) is assumed indpendent of the solvent conditions. [d] Protein concentration = 116 μM; CO concentration = 278 μM; $E_a = 0$ kcal/mol. [e] Protein concentration = 128 μM; CO concentration = 345 μM; E_a = 0.95 kcal/mol. [f] Protein concentration = 134 μM; CO concentration = 402 μM; E_a = 5.3 kcal/mol.

where the second term in parentheses normalizes the spectrum to the fraction of deoxyhemes present in the sample as determined from the amplitudes of V_1. The total deoxy spectral change in relaxation l, normalized to the concentration of the initial photoproduct, is then defined by $PS_l(\lambda) - PS_{l+1}(\lambda)$. The amplitude of the spectral change in the first relaxation (normalized by setting the total fitted amplitude of the spectral change at −5 °C in 75% glycerol/water to 1) is 0.55 and was assumed to be independent of the solvent conditions. The amplitudes of the deoxy spectral changes observed in the second and third relaxations are plotted in Figure 5d,e. The spectral changes observed for the second process increase in amplitude with decreasing temperature in each solvent, while the spectral changes associated with the third relaxation vary in both sign and magnitude when the solvent composition is altered. The spectral changes associated with the third relaxation are small (<15% of the total spectral change) and were not observed by Lambright et al. (1991) in experiments carried out on *human* Mb in 75% glycerol/water. Since we have considered only two SVD components in this analysis and have assumed that the amplitude of the first component is proportional to the fraction of deoxyhemes, the wavelength dependence of the deoxy spectral change in each of the relaxations is described by U_2. There are no deoxy spectral changes in the fourth relaxation, and the amplitude α_{24} corresponds entirely to ligand rebinding. Singular value decomposition of all the spectra in this relaxation yields a single component that corresponds to bimolecular rebinding to the relaxed deoxy conformation with higher order components that are less than 0.4%. In other words, protein conformational relaxation is complete prior to the bimolecular rebinding step.

The most striking result obtained from this empirical analysis of the kinetics of ligand rebinding and deoxy spectral

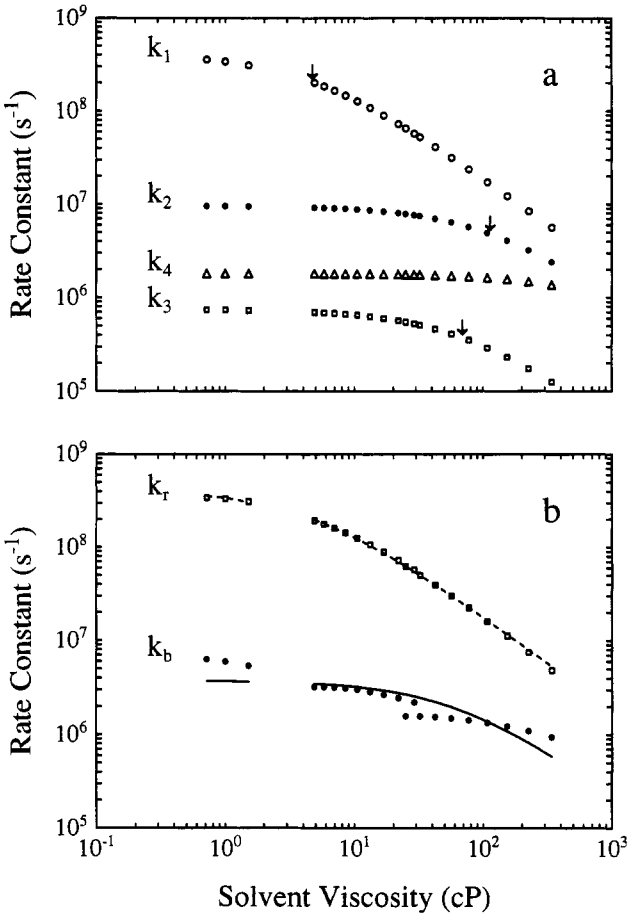

FIGURE 4: Dependence of the relaxation rates obtained from the empirical fit (eq 14) on solution viscosity. (a) The plotted values are the rate constants at 20 °C, obtained using eq 4 and the parameters in Table 1. The arrows indicate the values of σ that characterize the viscosity dependence of each of the relaxations. The bimolecular rebinding rate from the solvent, k_4, has units of M^{-1} s^{-1}; the corresponding σ is $>10^3$ cP. (b) The plotted values are the rates for protein conformational change (k_r) and the initial ligand-binding step (k_b) at 20 °C, estimated from the empirical fit. k_1 in eq 14 may be approximated as $k_1 \approx k_b + k_r$ and the rebinding amplitude in the first relaxation as $\alpha_{11}/\Sigma\alpha_{1k} \approx k_b/(k_b + k_r)$. k_b and k_r, calculated from the empirically determined k_1 and α_{1l}, are plotted as a function of the solvent viscosity. The lines through the data points are a fit using eq 4 with σ = 64 cP and $E_0 \simeq 0$ kcal/mol for k_b and σ = 4.4 cP and E_0 = 0.25 kcal/mol for k_r.

changes is that the first relaxation, which includes the largest deoxy spectral changes, depends strongly on solution viscosity (Figure 4a). The fitted relaxation rates for this process are dominated by the deoxy spectral change and therefore provide a very good first approximation to the rates for the protein conformational change. More accurate values are obtained when the contributions of ligand binding to this relaxation have been removed (Figure 4b). Both representations, when described by eq 4, yield a value for σ of about 4 and a small activation energy ($E_0 < 0.25$ kcal/mol) so that nearly all of the decrease in the rate observed at low temperature results from the increase in viscosity. This result depends critically on the assumption that the amplitude of the initial deoxy spectral change is independent of conditions but does not depend on the other assumptions used in empirically characterizing this process. In particular, neither the parametrization of this process as a stretched exponential nor the use of eq 4 to describe the viscosity dependence are essential. Similar results are obtained when this relaxation is fitted as an exponential (β_1 = 1) (Ansari et al., 1992) and when the

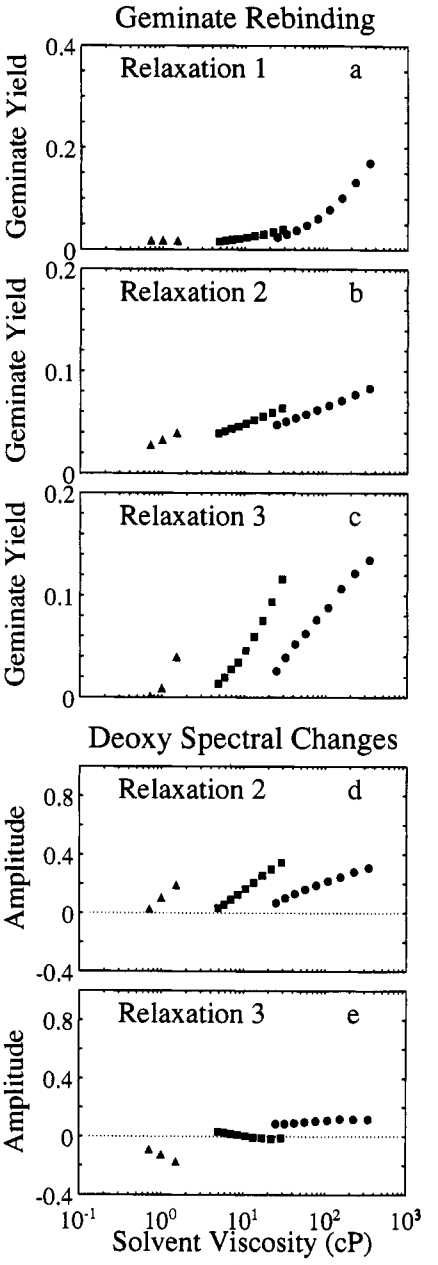

FIGURE 5: Fraction of total ligand rebinding and amplitudes of spectral changes obtained for each relaxation from the empirical fit. The first three panels (a–c) show the fractional ligand-rebinding yields for relaxations 1–3 obtained from the fits: (a) geminate yields for the first, stretched exponential process, α_{11}, (b) geminate yields for the second exponential process, α_{12}, and (c) geminate yields for the third exponential process, α_{13}. The corresponding amplitude for bimolecular rebinding is given by α_{14} in Table 1. (d and e) Amplitude of deoxy spectral changes in processes 2 and 3, calculated from eq 15. The amplitudes of the spectral changes have been normalized such that the total spectral amplitude at −5 °C in 75% glycerol/water is 1. The normalized amplitude of the spectral change in the first process, which was assumed to be independent of solvent and temperature, is 0.55.

viscosity dependence of the rate is empirically described by $\eta^{-\kappa}$.

A Minimal Model. The principal results of the SVD and the empirical analysis of the kinetic data (Figures 2–5, Table 1) are (i) that there are at least two deoxyheme spectra and therefore at least two deoxymyoglobin protein conformations, (ii) that protein conformational changes occur with viscosity-dependent rates on the same time scale as geminate rebinding, and (iii) that kinetic progress curves corresponding to both ligand rebinding and protein conformational changes prior to

the bimolecular rebinding phase are nonexponential. An empirical description of the geminate kinetics under all conditions reported in the present study requires one stretched exponential which describes the bulk of the conformational relaxation and two exponential relaxations which describe the remainder of the geminate kinetics. Even in water, where we previously reported geminate rebinding to take place in a single exponential relaxation (Henry et al., 1983a), the improved signal-to-noise ratio in the current experiments shows that geminate rebinding is nonexponential (Figure 5). Nonexponential geminate rebinding in water has also been observed by Champion and co-workers (Tian et al., 1992).

Our approach has been to explain the data with the simplest possible *chemical kinetic* model that contains all of the major physical concepts. Chemical kinetic models assume that there are well-defined intermediates that interconvert via exponential time courses. We recognize at the outset that this is probably an oversimplification and that a more realistic description may be required which permits, for example, nonexponential protein relaxation. Nevertheless, the approach of chemical kinetics appears to us to be a necessary first step. The model that we have chosen to present here may be considered a *minimal* model because it contains the fewest number of intermediates consistent with the idea that there are multiple protein conformations and multiple geminate states:[1]

$$\begin{array}{ccccccc} Mb^*CO & \rightleftharpoons & Mb^*{:}CO & \rightleftharpoons & Mb^*{::}CO & \rightleftharpoons & Mb^* + CO \\ \updownarrow & & \updownarrow & & \updownarrow & & \updownarrow \\ MbCO & \rightleftharpoons & Mb{:}CO & \rightleftharpoons & Mb{::}CO & \rightleftharpoons & Mb + CO \end{array}$$

$$\begin{array}{ccccccc} A^* & \rightleftharpoons & B^* & \rightleftharpoons & C^* & \rightleftharpoons & S^* \\ \updownarrow & & \updownarrow & & \updownarrow & & \updownarrow \\ A & \rightleftharpoons & B & \rightleftharpoons & C & \rightleftharpoons & S \end{array} \qquad (16)$$

In order to facilitate comparison with previous analyses, we use the notation of Frauenfelder and co-workers, in which A refers to the state with CO bound, B to the state with CO in the heme pocket, C to an additional geminate state, and S to the state with CO in the solvent. In this model, Mb* and Mb have distinct deoxyheme spectra that are independent of the position of the ligand in the molecule. Mb* is assumed to be the fast rebinding species and Mb the slow rebinding species; the ligand-binding rate B* $\rightarrow$ A* is therefore constrained to be greater than B $\rightarrow$ A. The basic idea of the model is that at least part of the spectral changes are due to the transition from the fast rebinding conformation Mb* to the slow rebinding conformation Mb. The model does not require that the liganded and unliganded protein conformations be identical but implies that any conformational changes between A* and B*, or between A and B, are much faster than the rates of ligand rebinding.

The minimal model (eq 16) is consistent with the known facts. The infrared spectra of the bound CO show at least three distinct bands, which are assumed to correspond to different conformations of the protein. The equilibrium populations of the protein molecules corresponding to these conformations depend upon temperature, pressure, and pH (Ansari et al., 1986; Iben et al., 1989; Hong et al., 1990). At the temperatures reported in this study, only two of the three conformations, designated by Frauenfelder and co-workers as A_1 and A_3, are significantly populated; the populations of A_1 and A_3 are approximately 75% and 25%, respectively; the population of A_0 is less than 4%. Ligand-binding studies at low temperatures using infrared spectroscopy show that the photoproduct of A_1 rebinds faster than that of A_3 (Ansari et al., 1987); there is, therefore, a possible correspondance between A* and A_1 and between A and A_3. In addition, there is both experimental and theoretical evidence for more than one geminate state. Austin and co-workers (Hong et al., 1991) found that the infrared spectrum of the photodissociated CO broadens and becomes undetectable in less than 50 ns above 250 K. This broadening presumably results from heterogeneity in the environment of the CO, as might be expected if it migrated to different parts of the protein. The molecular dynamics calculations of ligand motion through the protein by Elber and Karplus (1990) suggest that there is a finite probability of ligands returning to the pocket immediately adjacent to the heme before leaving the protein. Our minimal model ignores rebinding from what Traylor, Magde, and co-workers call the "contact pair" (Jongeward et al., 1988; Traylor et al., 1992). The contact pair may be viewed as the initial geminate state in which there are no intervening atoms between the heme iron and the ligand. Picosecond rebinding studies suggest that CO may be a unique ligand in that, unlike nitric oxide, oxygen, imidazole, or alkyl isocyanides, it escapes from this potential well before any ligand rebinding takes place. The escape rate has been estimated from molecular dynamics simulations to be about 25 ns^{-1} (Schaad et al., 1993).

Before exploring the model in detail, we first ask whether all of the spectral changes concurrent with the geminate-rebinding phase can be derived from "kinetic hole burning", i.e., an apparent change in the photoproduct spectrum due to rebinding alone without any interconversion between the two conformers prior to the bimolecular phase. To carry out a fit to the data, we assume that the interconversion between the two protein conformations is slow compared to the geminate-rebinding kinetics but that the two conformations can equilibrate prior to ligand rebinding from the solvent. To accomplish this, the rate constants for the interconversion of the B and C states (i.e., B* $\rightleftharpoons$ B and C* $\rightleftharpoons$ C) were constrained to be less than 10^4 s^{-1}. The equilibrium constant between the liganded conformations A* and A, which determines the relative initial populations of the two photodissociated species, was assumed to be solvent independent and was varied as a parameter in the fit. Small differences in the spectra of the deoxyhemes at long times were parametrized by assuming that the equilibrium between the two deoxy conformations is solvent dependent. We find that the equilibrium population of the two deoxy species as a function of the solvent changes by less than 7%. Any spectral differences between the liganded conformations are assumed to be smaller than the significant components retained from the SVD analysis and are therefore ignored.

There are enough geminate states in the model to adequately describe the ligand-binding kinetics. However, since the deoxy spectral changes in a kinetic hole burning model arise from differential depletion of the two conformers, the ligand-binding rates and amplitudes that describe the spectra of the deoxy species have to simultaneously satisfy the constraints imposed by the rate and amplitude for the spectral changes. A Monte Carlo search in parameter space produced a single minimum, and the results of the fit are shown in Figure 6. The model fits both the kinetics of ligand rebinding and the kinetics of

[1] We know from our empirical analysis of the data shown in Figures 2 and 3 that an accurate description at low temperatures and high solvent viscosities requires four exponential relaxations. From a purely phenomenological point of view, a minimum of five species are required to fit the data: a liganded state, an unliganded state with the ligand in the solvent, and three geminate intermediates. Consequently, a kinetic model with two conformations and one geminate state for each conformation is insufficient to fit the data.

the deoxy spectral changes very well. The fitted value of the fraction of fast rebinding molecules (Mb*) is about 26%. This result is consistent with the relatively small fraction of ligands which rebind synchronously with the major changes in the deoxy spectrum. However, a major problem is encountered with this fit; in order to explain the amplitude of the observed spectral changes, the deoxy spectrum of Mb* must be very different from that of relaxed deoxymyoglobin. As shown in Figure 6e, Mb* exhibits a double-peaked Soret band. To our knowledge, such a double-peaked Soret band has never been observed for a heme complex. In addition, in order to explain the decrease in the observed amplitude of the deoxy spectral change as the viscosity is lowered, the model predicts solvent-dependent geminate rebinding with more than 10% molecules having rebound in water within 10 ns (Figure 6d). This is inconsistent with measurements of the absolute quantum yield of 0.97 in microsecond experiments (Schuresco & Webb, 1978). We conclude, on the basis of the distorted Soret spectrum and the large amplitude for subnanosecond geminate rebinding in water, that it is unlikely that the spectral changes observed in the geminate phase result exclusively from kinetic hole burning and that protein conformational relaxation must take place on the same time scale as geminate rebinding.[2]

We can now proceed to examine the model with no constraints on the rate of interconversion of the two conformations. The equilibrium constant between the two liganded conformations, which determines the initial distribution of the photodissociated species, was varied systematically to determine its effect on the fit. Most of the rate parameters and the spectra obtained from the fit were found to be insensitive to the value chosen for the equilibrium constant; we therefore fixed it from the infrared measurements, i.e., $[A^*]/[A] = [A_1]/[A_3] = \exp(0.48/RT)$ (Ansari et al., 1987). Exploration of parameter space with the Monte Carlo procedure, in which the fits were started with random initial values of the parameters, resulted in six fits representing at least three different regions in the parameter space with similar values for the χ^2. The fit of this model to the data with the lowest value of χ^2 is shown in Figure 7 for the 20 °C data; the model fits the major features of the data very well and produces reasonable spectra for the two conformations. The misfits in the kinetics of deoxy spectral changes could, of course, be reduced by adding an additional tier of conformational states at the expense of increasing the parameter set. We have chosen not to do so since the parameter set is already very large and highly correlated.

Because of the large number of parameters in the model (14 independent rate constants, 9 values of σ, and 14 activation energies), many of the parameters were not well determined, and different minimia with very different kinetic parameters were found with similar values for χ^2. The fitted rate parameters obtained from the three best fits are summarized

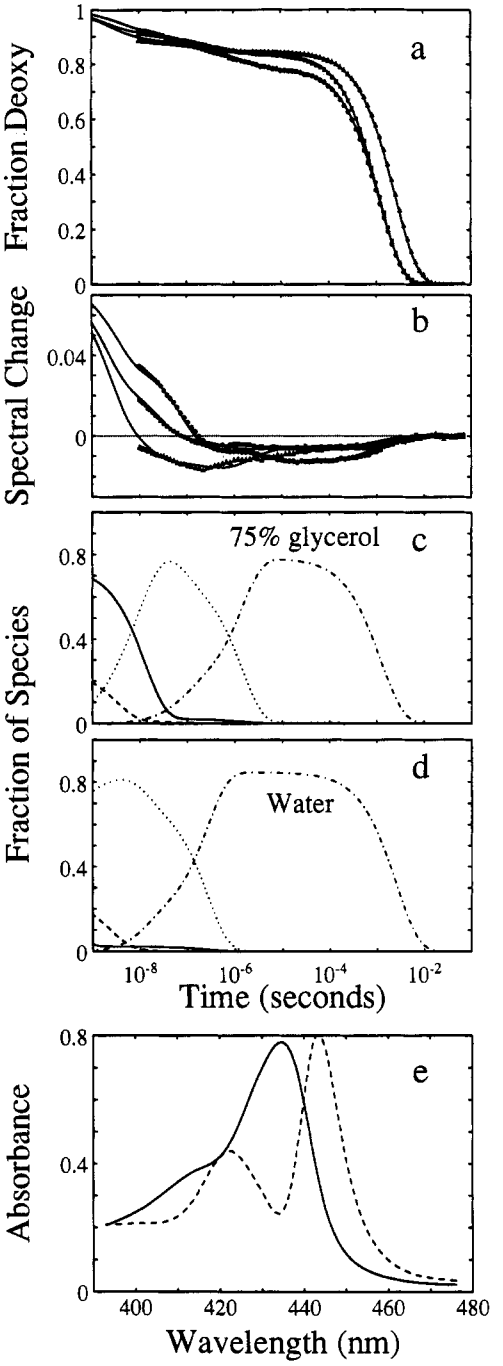

FIGURE 6: Fit to the kinetic hole burning model. The data fitted were for (Δ) water at 5, 20, and 35 °C, (□) 50% glycerol/water at −5–35 °C in 5 °C steps, and (○) 75% glycerol/water at −5 to 35 °C in 5 °C steps (χ^2 = 13). The fits shown are to the data at 20 °C: (a) fits to V_1 obtained using eq 16, (b) fits to V_2 obtained using eq 16, (c and d) fractional populations of the deoxy states B* (– – –), B (—), C* + C (...), and S* + S (– · –) at 20 °C in (c) 75% glycerol/water and (d) water, and (e) absorption spectra of deoxy species Mb* (– – –) and Mb (—).

in Figure 8b–d. The main deoxyheme spectral change in the time window between 10 and 300 ns (B* → B) results from a protein conformational change with a rate that is well determined, as evidenced by the narrow distribution of rate constants, activation energies, and σ's from the fits. The rate of this process is 8.6 (±4.1) × 10^6 s^{-1} in 75% glycerol/water solution at 20 °C, its activation energy is about 3 (±1) kcal/mol, and its viscosity dependence is characterized by σ = 1.7 (+2.6, −1) cP. The geminate-rebinding rate for the faster rebinding molecules (B* → A*) is 2.4 (±0.6) × 10^6 s^{-1} with

[2] We explored the kinetic hole burning idea further by carrying out a fit in which the equilibrium constant between the liganded conformations was fixed from the equilibrium constant measured in the infrared experiments, i.e., $[A^*]/[A] = [A_1]/[A_3] = \exp(0.48/RT)$ (Ansari et al., 1987). This more constrained model, with one less parameter, cannot simultaneously fit both the ligand-rebinding kinetics and the kinetics of the deoxy spectral changes (the χ^2 increased by a factor of 3). The main reason for the misfit is that the relative populations of the two conformers were essentially reversed in this fit; the value for the fraction of rapidly rebinding photoproduct (Mb*) as predicted by the infrared measurements is about 70%, which is the exact opposite of the value for the populations predicted by the model if the equilibrium constant between A* and A is allowed to vary. Furthermore, the major problems remain, i.e., more than 10% geminate rebinding in water within 10 ns and a double-peaked Soret band for the slow rebinding Mb.

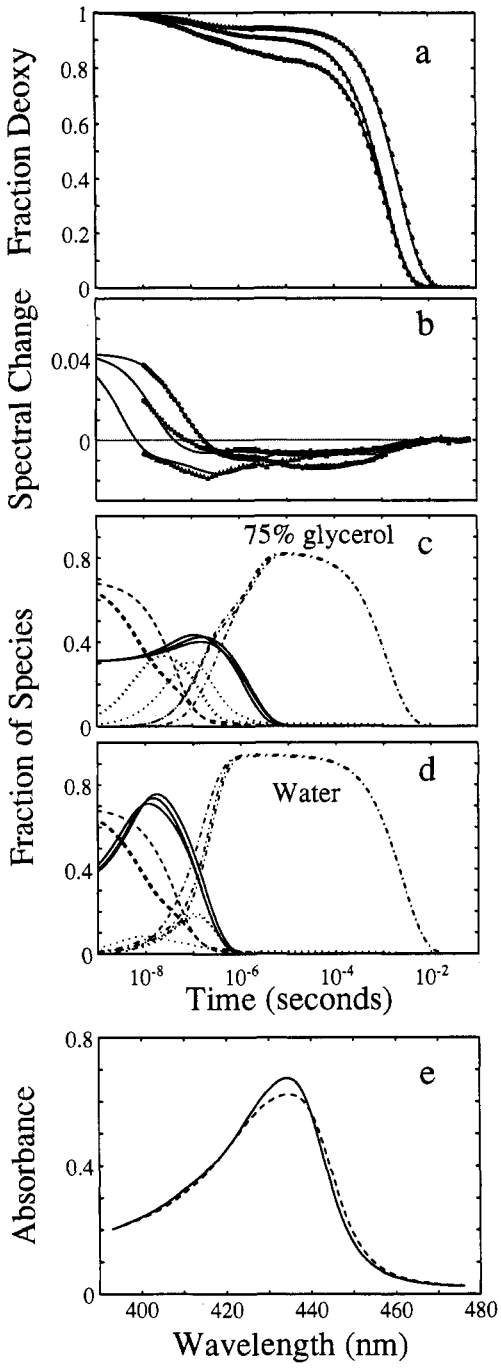

FIGURE 7: Fit to the conformational relaxation model. The data fitted were for (△) water at 5, 20, and 35 °C, (□) 50% glycerol/water at −5 to 35 °C in 5 °C steps, and (○) 75% glycerol/water at −5 to 35 °C in 5 °C steps (χ^2 = 14.4). The fits shown are to the data at 20 °C: (a) fits to V_1 and (b) fits to V_2 obtained using eq 16. (c and d) Fractional populations of the deoxy states B* (– – –), B (—), C* + C (...), and S* + S (– · –) at 20 °C in (c) 75% glycerol/water and (d) water. The spread in the populations is from the three best fits with comparable χ^2 of 14.4, 16.8, and 16.8. (e) Absorption spectra of deoxy species Mb* (– – –) and Mb (—).

an activation energy E_0 = 2.8 (±1.5) kcal/mol and a relatively small viscosity dependence ($\sigma > 10^3$). The geminate-rebinding rate for the slower rebinding molecules (B → A) is about a factor of 100 smaller and is less well determined in this model since the dissociated ligand can either rebind directly or rebind by equilibrating with the faster rebinding species. Owing to the multiple pathways available to the system, the rate parameters for most of the other steps are correlated and not very well determined. Exceptions are the entry and exit rates

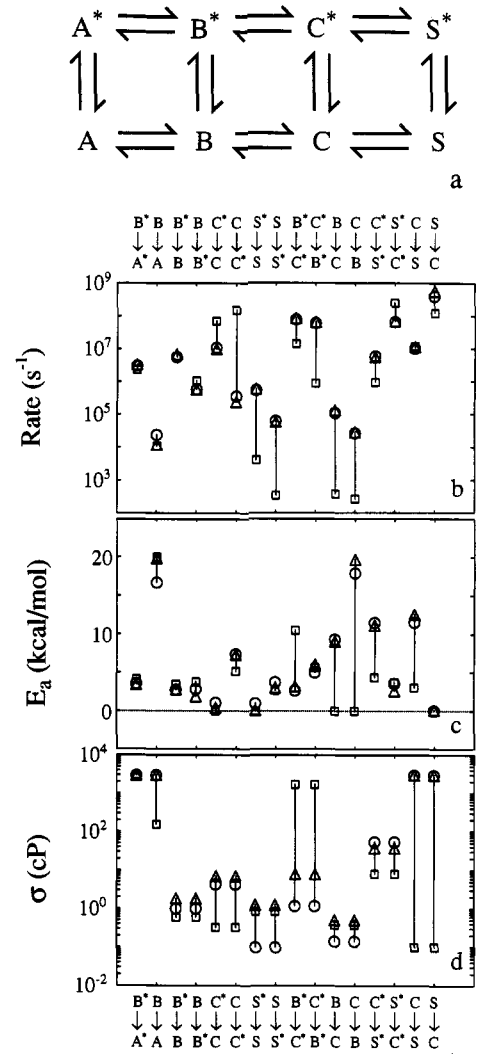

FIGURE 8: Rate parameters obtained from the conformational relaxation model fit to the data: (a) conformational relaxation model (eq 16), (b) rate constants at 20 °C in 75% glycerol/water, (c) corresponding activation energies, and (d) values of σ for each of the steps indicated in (a). The rate parameters plotted are for the three best fits obtained from the Monte Carlo search with different starting values for the parameters as described in Materials and Methods: (□) χ^2 = 14.4, (○) χ^2 = 16.8, and (△) χ^2 = 16.8. The other three fits obtained from the Monte Carlo procedure have values of χ^2 = 26.8, 28.9, and 31.3. The average values of the parameters quoted in the text were calculated using the values from all the fits weighted by $1/\chi^2$ and differ slightly from the average values obtained from the figure. The units for the rate constants k(S → C) and k(S* → C*) are M^{-1} s^{-1}.

from the solvent: the average exit rate (C* → S*, C → S, averaged over the two conformations) is $\langle k_{cs} \rangle$ = 5 (+7.5, −3) × 10^6 s^{-1}, $\langle E_{cs} \rangle$ = 9.4 (±3.6) kcal/mol, and the average entry rate (S* → C*, S → C) is $\langle k_{sc} \rangle$ = 1.1 (+2.4, −0.75) × 10^8 M^{-1} s^{-1}, $\langle E_{sc} \rangle$ = 1.7 (±1.9) kcal/mol.

Consideration of the values of the viscosity-dependent parameter σ gives some insight into the nature of the kinetic steps of the model. The large value of σ (≈10^3) for the heme-rebinding steps, indicating a small viscosity dependence, suggests that the protein motions which influence ligand-binding dynamics do not displace solvent atoms and are therefore localized to the interior of the protein. In contrast, the small value of σ (<10) for all of the conformational rates between Mb* and Mb, indicating a large viscosity dependence, suggests that the conformational change displaces solvent atoms. The small value of σ for the conformational rates is consistent with the idea that the conformational change is a

global displacement of the protein atoms on the proximal side of the heme, as depicted in Figure 1.

It is difficult to draw any conclusions about the viscosity dependence of the individual steps describing the motion of the ligand, since the value of σ depends upon the detailed pathway which varies considerably from one fit to another. One can, however, calculate the average viscosity dependence for the entry and exit steps by averaging over the equilibrium populations of the two deoxy conformations. The value of $\langle\sigma_{cs}\rangle$ ($=\langle\sigma_{sc}\rangle$) thus obtained is about 80 cP, suggesting a small viscosity dependence for this step. We should point out, in this regard, that if the viscosity dependence for the ligand motion steps is a result of viscosity-dependent transitions between conformational substates that have not been explicitly included in our model and that underlie the two conformations, then, as discussed earlier, a preexponential factor of the form A/η^{κ} (eq 11) may be more appropriate for these steps (Beece et al., 1980; Agmon & Hopfield, 1983; Agmon & Kosloff, 1987; Zwanzig, 1992).

One of the difficulties in fitting the data was to account for the nonmonotonic change in the deoxyheme optical spectrum. This complex behavior, particularly in water between about 100 ns and 10 μs (Figure 2f), suggests that structural changes other than the global displacement of atoms on the proximal side of the heme are responsible for the spectral changes. One such structural change might correspond to the process observed by photoacoustic calorimetry. In the photoacoustic calorimetric measurements, an endothermic process was observed at about 700 ns subsequent to the completion of geminate rebinding. This relaxation was interpreted as resulting from a conformational change which permits the salt bridge between Arg-45 and the propionate side chain of the heme to reform (Westrick et al., 1987; Westrick & Peters, 1990). The initial breakage of the salt bridge was not resolved but occurred in less time than the time resolution of the measurement, which was about 50 ns.

A major advantage of measuring multiwavelength kinetics is that kinetic modeling generates the spectra of the individual molecular species. We have already used the spectra to help rule out a pure kinetic hole burning model. Figure 7b shows the deoxyheme spectra of the two deoxymyoglobin conformations generated from fitting the data with the minimal model. The fast rebinding species (Mb*) exhibits a deoxyheme spectrum which is red-shifted, is broader, and has a lower peak extinction coefficient than the slow rebinding species (Mb). The differences between the spectra are similar to those observed in kinetic hole burning experiments (Ormos et al., 1990). These are also similar to the spectral differences that are observed between the fast rebinding R and slow rebinding T conformations of hemoglobin (Sawicki & Gibson, 1976; Hofrichter et al., 1983; Jones et al., 1992) as well as the differences between the immediate photoproduct and the relaxed species of hemoglobin that exist prior to the quaternary conformational change from R to T. The X-ray structures of deoxyhemoglobin in both the R and T conformations are known, and the iron is more displaced from the heme plane in the T conformation (Perutz et al., 1987). Another interesting comparison with hemoglobin is that the geminate yield of hemoglobin is much larger—40% for R-state hemoglobin in water compared to about 6% for myoglobin (Figure 5a) in water. In hemoglobin, the relaxation rate is also much longer for the initial relaxation—20 ns (Jones et al., 1992) compared to about 2 ns (Figure 4a). These results suggest that the much higher geminate yield in R-state hemoglobin is due to a slower conformational relaxation, allowing more time for ligands to rebind to the faster binding tertiary conformation.

SUMMARY AND CONCLUSIONS

The principal aim of this study has been to experimentally characterize the kinetics of conformational changes following photodissociation of the heme–CO complex in myoglobin and to determine how these conformational changes influence the kinetics of ligand rebinding. As was observed earlier (Lambright et al., 1991; Ansari et al., 1992; Tian et al., 1992), spectral changes of the deoxyheme photoproduct occur on the same time scale as geminate ligand rebinding. These spectral changes are similar to what have been observed for hemoglobin, where comparisons with X-ray structures suggest that they arise from a change in the displacement of the iron from the heme plane (Murray et al., 1988). Since the position of the iron is influenced by the protein conformation via its covalent link to the proximal histidine, we attribute changes in the spectrum to changes in the protein conformation.

There are two limiting interpretations of the spectral changes in terms of conformational changes. In one, there are two (or more) conformations of the protein that are populated immediately after photolysis and that do not interconvert during ligand rebinding. If they have different rates of geminate ligand rebinding and different deoxyheme spectra, a deoxyheme spectral change concurrent with ligand rebinding necessarily results from the differential depletion of one of the conformers. This is known as kinetic hole burning. The deoxyheme spectral change observed during the rebinding of CO to a mixture of the fast rebinding R and slow rebinding T conformations of hemoglobin is a classic example (Hofrichter et al., 1983, 1985). A second limiting interpretation is that only a single protein conformation is populated upon photolysis, which then undergoes a conformational change. This has been called conformational relaxation. We have ruled out a *pure* kinetic hole burning model because the spectra produced by such a model are implausible (Figure 6). The spectral changes must therefore be due at least in part to conformational relaxation.

Our problem, then, was to develop the simplest model which contained conformational relaxation and could also explain the nonexponential geminate rebinding. The model is the minimal model that incorporates all of the major features of myoglobin kinetics at ambient temperatures, including a fast and slow binding conformation, Mb* and Mb, and two geminate states for each conformation (eq 16). In the context of this model, the conformational relaxation is understood to be the interconversion of Mb* and Mb conformations. Because of the large number of parameters in the model, it was not possible to uniquely determine all of the rate constants (Figure 8). Nevertheless, several important results emerged. First, the model indicates that all three effects that have been discussed in the past—multiple conformations (in this case two) rebinding with different rates, conformational relaxation, and multiple geminate states—can contribute to the nonexponential rebinding. Second, the protein relaxation, which in this model is the transition from state B* to B (eq 16), substantially decreases the rate of geminate rebinding as envisaged in earlier work (Agmon & Hopfield, 1983; Henry et al., 1983b; Hofrichter et al., 1985; Friedman, 1985; Steinbach et al., 1991). The magnitude of this decrease is not well determined at all temperatures but is of the order of 100 at 20 °C (Figure 8).

Another major result from the modeling is that the protein relaxation rates ($k(B^* \rightarrow B)$, $k(C^* \rightarrow C)$, and $k(S^* \rightarrow S)$)

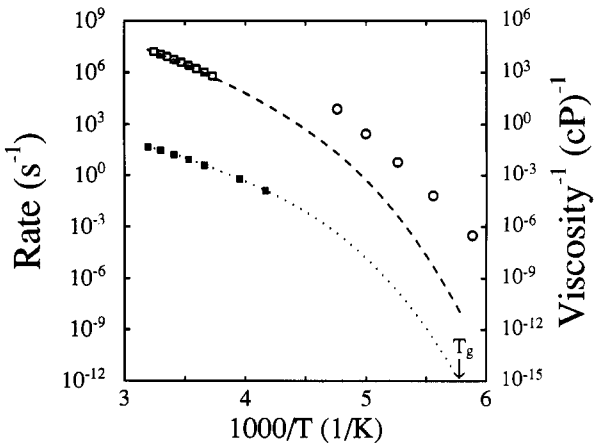

FIGURE 9: Comparison of measured rates for myoglobin conformational relaxations and viscosity of glycerol/water solvent. (○) Conformational relaxation rate in myoglobin from Steinbach et al. (1990). The relaxation rates were derived from a fit to the ligand-rebinding kinetics in 75% glycerol/water in the temperature range 160–210 K. (– – –) Conformational relaxation rate $k(B^* \rightarrow B)$ in 75% glycerol/water obtained from a fit to the model (eq 16). The values of the relaxation rates at low temperatures are obtained from eq 4, using the values of E_0 and σ obtained from the fit and the values of the viscosities indicated in the figure. The symbols (□) indicate the temperature range over which the measurements were made. (■) Inverse of the viscosities (in cP) for 80% w/w glycerol measured as a function of temperature (Newman, 1971). The viscosities at lower temperatures (dotted line) were estimated from an empirical description of the viscosities for various liquids as a function of the reduced temperature T_g/T where T_g is the glass-transition temperature of the solvent; the viscosities for a number of liquids at $T = T_g$ were shown to extrapolate to 10^{15} cP (Angell & Sichina, 1976). $T_g = 173$ K for 80% w/w glycerol was used in the calculation of the viscosities (Rasmussen & MacKenzie, 1971).

are strongly dependent on solvent viscosity, as was found in the empirical analysis (Ansari et al., 1992). In contrast, the geminate-rebinding rate exhibited almost no dependence on solvent viscosity. The dependence of the rate of protein relaxation on $1/\eta$ at high viscosities (eq 10) indicates an enormous slowing as the temperature is lowered toward the glass transition. Is this the relaxation postulated by Steinbach et al. (1991) to slow down geminate rebinding as the temperature is raised just above the glass transition? Figure 9 compares the rates determined from the model of eq 16 and extrapolated to low temperature with the rates obtained by Steinbach et al. from the fit to their ligand-rebinding data. The extrapolated rates are significantly slower than those of Steinbach et al., suggesting that there is a faster component to the protein relaxation that has not been resolved in our experiments. This faster component could very well be the relaxation observed by Anfinrud and co-workers (Lim et al., 1993). They described the shift in the near-infrared charge-transfer band at room temperature in water in the range 2 ps–3 ns with a sum of three exponential terms with time constants of 3.5 and 83 ps and 3.3 ns. The 3.3-ns time constant agrees well with the value of 4.7 ns obtained from the eigenvalue for the first relaxation predicted by the modeling. More recently, Anfinrud and co-workers (Jackson et al., 1994) have extended their measurements to longer times and have found that the protein relaxation appears to be a single continuous process from picoseconds to about 10 μs in 70:30 w/w glycerol/water mixtures.

A further comparison of the different measurements may be made by considering the amplitudes of the spectral changes observed in these experiments. This comparison is most easily made by discussing the observed spectral changes in terms of the frequency shifts associated with the spectral change, that is, the changes in the first moments of the observed spectra. Šrajer and Champion (1991) made an interesting observation that the maximum spectral shift between the photoproduct and the deoxy conformations, obtained from a comparison of the spectra at 10 K, is about 140 cm^{-1} in both the Soret and the near-infrared. Anfinrud and co-workers observed frequency shifts in the near-infrared band of approximately 100 cm^{-1} at 300 K and in the time range 2 ps–3 ns (Lim et al., 1993; Jackson et al., 1994). The frequency shift at ambient temperatures calculated from the spectral change shown in Figure 7 is only about 30 cm^{-1}, suggesting again that we have not fully resolved a large amplitude of the protein conformational changes even at the highest viscosities in our experiments.

The missing amplitude in our experiments is probably functionally significant and suggests that our estimate of a factor of 100 for the ratio of the rates $k(B^* \rightarrow A^*)/k(B \rightarrow A)$ should be regarded as a minimum value. The average rate of ligand rebinding from the pocket state B* extrapolated from low-temperature measurements prior to the Mb* → Mb relaxation postulated by Steinbach et al. (1991) is about $7 \times 10^7\ s^{-1}$, approximately 30-fold faster than the ligand rebinding rate $k(B^* \rightarrow A^*)$ obtained from our kinetic modeling, suggesting that the subnanosecond conformational relaxation does in fact decrease the rate of ligand rebinding. If the extrapolated rate of rebinding to the unrelaxed conformation of $7 \times 10^7\ s^{-1}$ is correct, the complete relaxation would decrease the geminate-rebinding rate by a factor of about 3000 (i.e., in the context of our model, $k(B^* \rightarrow A^*)/k(B \rightarrow A) = 3000$). Since we have attributed a decrease in the geminate-rebinding rate of a factor of 100 to a 30-cm^{-1} shift out of a possible 140-cm^{-1} shift in the Soret band, while only a factor of 30 is attributed to the initial 110 cm^{-1}, it would appear that there is a highly nonlinear relation between the frequency shift and the logarithm of the geminate-rebinding rate constant. This curvature is also apparent in the analysis of the low-temperature geminate-rebinding rates and the near-infrared spectra by Steinbach et. (1991).

It is interesting to note that these rather large changes in the rebinding rates are accomplished by such a small change in protein conformation (Figure 1). Is it possible that the X-ray structures are not revealing the conformational changes that occur in solution? The structure of the carbon monoxide complex was not determined from crystals grown as the carbon monoxide complex but was determined from crystals that were grown as metmyoglobin and then reduced with sodium dithionite in the presence of carbon monoxide (Kuriyan et al., 1986). The lattice forces could prevent tertiary conformational changes of myoglobin that would otherwise occur in solution, as has been suggested in ligand-binding studies of hemoglobin crystals (Rivetti et al., 1993).

The picture emerging is that our measurements have detected the final portion of the protein relaxation that begins on a picosecond time scale at room temperature. This protein relaxation is probably the same relaxation postulated by Frauenfelder and co-workers (Steinbach et al., 1991). It would appear that an important next step would be to obtain experimental data over even wider temperature, time, and wavelength ranges. This will be necessary to make the connection more clear among the data from our work as well as those of Boxer and co-workers (Lambright et al., 1991, 1993), Steinbach et al. (1991), and Anfinrud and co-workers (Lim et al., 1993; Jackson et al., 1994). It will also be necessary to develop additional spectral probes to define much more precisely the conformational changes responsible for the optical

changes. At present, we, like previous investigators, have envisaged that after photodissociation there is a very rapid (<300 fs) initial displacement of the iron associated with ligand photodissociation, as indicated by both optical absorption measurements (Martin et al., 1983) and molecular dynamics simulations (Henry et al., 1985; Petrich et al., 1991; Kuczera et al., 1993; Schaad et al., 1993). This is followed by a slower displacement associated with the rearrangement of protein atoms to accommodate the new heme conformation. This slower displacement occurs over a wide range of times, from picoseconds to nanoseconds in water at room temperature. It has been observed in some molecular dynamics simulations (Petrich et al., 1991; Kuczera et al., 1993) but not in others (Li et al., 1993; Schaad et al., 1993). Since ligand rebinding reverses the protein conformational change, the rate of rebinding decreases as the conformational relaxation proceeds, that is, rebinding to a conformation that is closer to that of the liganded molecule is faster than ligand rebinding to the relaxed deoxy conformation.

Although the modeling using a conventional chemical kinetic scheme has been extremely useful in showing that the data is consistent with the basic idea that protein relaxation slows down geminate rebinding (and in our view was a necessary first step in analyzing the kinetics), it may be both an oversimplification and misleading. Unlike the kinetics of the R and T conformations of hemoglobin, the description of the protein conformational kinetics of myoglobin in terms of well-defined kinetic intermediates may very well be an incorrect physical picture. The R and T conformations of hemoglobin have a different packing of the subunits with changes in the residues that interact between the subunits. The conformational changes in myoglobin (and the *tertiary* conformational changes in hemoglobin) are both more subtle and more complex, and a different approach is needed. Presumably, the nonexponential protein relaxation kinetics are somehow related to the complex potential energy hypersurface of the protein (its "rugged landscape"), as suggested by Frauenfelder et al. (1991). There is, however, no physical model of a protein or analogous system that can rigorously generate these kinetics.

ACKNOWLEDGMENT

We thank Peter Steinbach, Attila Szabo, and Robert Zwanzig for helpful discussions and Philip Anfinrud for sending us preprints of his work.

REFERENCES

Ackerman, E., & Berger, R. L. (1963) *Biophys. J. 3*, 493–505.
Agmon, N. (1988) *Biochemistry 27*, 3507–3511.
Agmon, N., & Hopfield, J. J. (1983) *J. Chem. Phys. 79*, 2042–2053.
Agmon, N., & Kosloff, R. (1987) *J. Phys. Chem. 91*, 1988–1996.
Alpert, B., El Mohsni, S., Lindqvist, L., & Tfibel, F. (1979) *Chem. Phys. Lett. 64*, 11–16.
Angell, C. A., & Sichina, W. (1976) *Ann. N. Y. Acad. Sci. 279*, 53–67.
Ansari, A., & Szabo, A. (1993) *Biophys. J. 64*, 838–851.
Ansari, A., Berendzen, J., Bowne, S. F., Frauenfelder, H., Iben, I. E. T., Sauke, T. B., Shyamsunder, E., & Young, R. D. (1985) *Proc. Natl. Acad. Sci. U.S.A. 82*, 5000–5004.
Ansari, A., DiIorio, E. E., Dlott, D. D., Frauenfelder, H., Iben, I. E. T., Langer, P., Roder, H., Sauke, T. B., & Shyamsunder, E. (1986) *Biochemistry 25*, 3139–3146.
Ansari, A., Berendzen, J., Brauenstein, D., Cowen, B. R., Frauenfelder, H., Hong, M. K., Iben, I. E. T., Johnson, J. B., Ormos, P., Sauke, T. B., Schulte, A., Steinbach, P. J., Vittitow, J., & Young, R. D. (1987) *Biophys. Chem. 26*, 337–355.
Ansari, A., Jones, C. M., Henry, E. R., Hofrichter, J., & Eaton, W. A. (1992) *Science 256*, 1796–1798.
Ansari, A., Jones, C. M., Henry, E. R., Hofrichter, J., & Eaton, W. A. (1993) *Biophys. J. 64*, 852–868.
Austin, R. H., Beeson, K. W., Eisenstein, L., Frauenfelder, H., & Gunsalus, I. C. (1975) *Biochemistry 14*, 5355–5373.
Bässler, H. (1987) *Phys. Rev. Lett. 58*, 767–770.
Beece, D., Eisenstein, L., Frauenfelder, H., Good, D., Marden, M. C., Reinisch, L., Reynolds, A. H., Sorensen, L. B., & Yue, K. T. (1980) *Biochemistry 19*, 5147–5157.
Campbell, B. F., Chance, M. R., & Friedman, J. M. (1987) *Science 283*, 373–376.
Catterall, R., Duddell, D. A., Morris, R. J., & Richards, J. T. (1982) *Biochim. Biophys. Acta 705*, 257–263.
Chernoff, D. A., Hochstrasser, R. M., & Steele, A. W. (1980) *Proc. Natl. Acad. Sci. U.S.A. 77*, 5606–5610.
Cordone, L., Cupane, A., Leone, M., & Vitrano, E. (1986) *Biophys. Chem. 24*, 259–275.
Cordone, L., Cupane, A., Leone, M., Vitrano, E., & Bulone, D. (1988) *J. Mol. Biol. 119*, 213–218.
Cornelius, P. A., Steele, A. W., Chernoff, D. A., & Hochstrasser, R. M. (1981) *Proc. Natl. Acad. Sci. U.S.A. 78*, 7526–7529.
Dasgupta, S., Spiro, T. G., Johnson, C. K., Dalickas, G. A., & Hochstrasser, R. M. (1985) *Biochemistry 24*, 5295–5297.
Duddell, D. A., Morris, R. J., & Richards, J. T. (1979) *J. Chem. Soc. Chem. Commun.* 75–76.
Duddell, D. A., Morris, R. J., & Richards, J. T. (1980a) *Biochim. Biophys. Acta 621*, 1–8.
Duddell, D. A., Morris, R. J., & Richards, J. T. (1980b) *Photochem. Photobiol. 31*, 479–484.
Elber, R., & Karplus, M. (1990) *J. Am. Chem. Soc. 112*, 9161–9175.
Findsen, E. W., Scott, T. W., Chance, M. R., & Friedman, J. M. (1985) *J. Am. Chem. Soc. 107*, 3355–3357.
Frauenfelder, H., Sligar, S. L., & Wolynes, P. G. (1991) *Science 254*, 1598–1603.
Friedman, J. M. (1985) *Science 228*, 1273–1280.
Friedman, J. M., & Lyons, K. B. (1980) *Nature 284*, 570–572.
Gavish, B. (1980) *Phys. Rev. Lett. 44*, 1160–1163.
Gavish, B. (1986) in *The Fluctuating Enzyme* (Welch, G. R., Ed.) pp 263–339, Wiley, New York.
Genberg, L., Richard, L., McClendon, G., & Miller, R. J. D. (1991) *Science 251*, 1051–1054.
Greene, B. I., Hochstrasser, R. M., Weisman, R. B., & Eaton, W. A. (1978) *Proc. Natl. Acad. Sci. U.S.A. 75*, 5255–5259.
Hänggi, P., Talkner, P., & Borkovec, M. (1990) *Rev. Mod. Phys. 62*, 251–341.
Hanson, J. C., & Schoenborn, B. P. (1981) *J. Mol. Biol. 153*, 117–146.
Henry, E. R., & Hofrichter, J. (1992) *Methods Enzymol. 210*, 129–192.
Henry, E. R., Sommer, J. H., Hofrichter, J., & Eaton, W. A. (1983a) *J. Mol. Biol. 166*, 443–451.
Henry, E. R., Hofrichter, J., Sommer, J. H., & Eaton, W. A. (1983b) in *Hemoglobins: structure and function* (Schnek, A. G., & Paul, C., Eds.) pp 193–203, Edition de l'Universite de Bruxelles, Brussels.
Henry, E. R., Levitt, M., & Eaton, W. A. (1985) *Proc. Natl. Acad. Sci. U.S.A. 82*, 2034–2038.
Hindmarsh, A. C. (1983) in *Scientific Computing* (Stepleman, R. S., et al., Eds.) pp 55–64, North-Holland, Amsterdam.
Hofrichter, J., Henry, E. R., Sommer, J. H., & Eaton, W. A. (1983) *Proc. Natl. Acad. Sci. U.S.A. 80*, 2235–2239.
Hofrichter, J., Henry, E. R., Sommer, J. H., Deutsch, R., Ikeda-Saito, M., Yonetani, T., & Eaton, W. A. (1985) *Biochemistry 24*, 2667–2679.
Hofrichter, J., Henry, E. R., Szabo, A., Murray, L. P., Ansari, A., Jones, C. M., Coletta, M., Falcioni, G., Brunori, M., & Eaton, W. A. (1991) *Biochemistry 30*, 6583–6598.
Hofrichter, J., Henry, E. R., Ansari, A., Jones, C. M., Deutsch, R. M., & Sommer, J. (1994a) *Methods Enzymol.* (in press).

Hong, M. K., Brauenstein, D., Cowen, B. R., Frauenfelder, H., Hong, M. K., Iben, I. E. T., Mourant, J. R., Ormos, P., Scholl, R., Schulte, A., Steinbach, P. J., Xie, A.-H., & Young, R. D. (1990) *Biophys. J. 58*, 429–436.

Hong, M. K., Shyamsunder, E., Austin, R. H., Gerstman, B. S., & Chan, S. S. (1991) *Phys. Rev. Lett. 66*, 2673–2676.

Iben, I. E. T., Brauenstein, D., Doster, W., Frauenfelder, H., Hong, M. K., Johnson, J. B., Luck, S., Ormos, P., Sauke, T. B., Schulte, A., Steinbach, P. J., Xie, A.-H., & Young, R. D. (1989) *Phys. Rev. Lett. 62*, 1916–1919.

Jackson, T. A., Lim, M., & Anfinrud, P. A. (1994) *Chem. Phys. 180*, 131–140.

Janes, S. M., Dalickas, G. A., Eaton, W. A., & Hochstrasser, R. M. (1988) *Biophys. J. 54*, 545–549.

Jones, C. M., Ansari, A., Henry, E. R., Christoph, G. W., Hofrichter, J., & Eaton, W. A. (1992) *Biochemistry 31*, 6692–6702.

Jongeward, K. A., Magde, D., Taube, D. J., Marsters, J. C., Traylor, T. G., & Sharma, V. S. (1988) *J. Am. Chem. Soc. 110*, 380–387.

Kirkpatrick, S., Gelatt, C. D., & Vecchi, M. P. (1983) *Science 220*, 671–680.

Kramers, H. A. (1940) *Physica (Amsterdam) 7*, 284–304.

Kuriyan, J., Wilz, S., Karplus, M., & Petsko, G. (1986) *J. Mol. Biol. 192*, 133–154.

Kuczera, K., Lambry, J. L., Martin, J. L., & Karplus, M. (1993) *Proc. Natl. Acad. Sci. U.S.A. 90*, 5805–5807.

Lambright, D. G., Balasubramanian, S., & Boxer, S. G. (1991) *Chem. Phys. 158*, 249–260.

Lambright, D. G., Balasubramanian, S., & Boxer, S. G. (1993) *Biochemistry 32*, 10116–10124.

Leone, M., Cordone, L., Vitrano, E., & Cupane, A. (1987) *Biopolymers 26*, 1769–1779.

Li, H., Elber, R., & Straub, J. E. (1993) *J. Biol. Chem. 268*, 17908–17916.

Lim, M., Jackson, T. A., & Anfinrud, P. A. (1993) *Proc. Natl. Acad. Sci. U.S.A. 90*, 5801–5804.

Loncharich, R. J., Brooks, B. R., & Pastor, R. W. (1992) *Biopolymers 32*, 523–535.

Lyons, K. B., & Friedman, J. M. (1982) in *Hemoglobin and Oxygen Binding* (Ho, C., et al., Eds.) pp 333–338, Elsevier North Holland, New York.

Martin, J. L., Migus, A., Poyart, C., Lecarpentier, Y., Astier, R., & Antonetti, A. (1983) *Proc. Natl. Acad. Sci. U.S.A. 80*, 173–177.

Marquardt, D. W. (1963) *J. Soc. Ind. Appl. Math. 11*, 431–441.

McCammon, J. A., Wolynes, P. G., & Karplus, M. (1979) *Biochemistry 18*, 927–942.

McKinnie, R. E., & Olson, J. S. (1981) *J. Biol. Chem. 256*, 8928–8932.

Metropolis, N., Rosenbluth, A. W., Rosenbluth, M. N., Teller, A. H., & Teller, E. (1953) *J. Chem. Phys. 21*, 1087–1092.

Morris, R. J., Duddell, D. A., & Richards, J. T. (1982) in *Hemoglobin and Oxygen Binding* (Ho, C., et al., Eds.) pp 339–343, Elsevier North Holland, New York.

Murray, L. P., Hofrichter, J., Henry, E. R., & Eaton, W. A. (1988) *Biophys. Chem. 29*, 63–76.

Nienhaus, G. U., Mourant, J. R., & Frauenfelder, H. (1992) *Proc. Natl. Acad. Sci. U.S.A. 89*, 2902–2906.

Nobbs, C. L. (1966) in *Hemes and Hemoproteins* (Chance, B., Estabrook, R. W., & Yonetani, T., Eds.) pp 143–148, Academic Press, New York.

Ormos, P., Ansari, A., Braunstein, D., Cowen, B. R., Frauenfelder, H., Hong, M. K., Iben, I. E. T., Sauke, T. B., Steinbach, P. J. & Young, R. D. (1990) *Biophys. J. 57*, 191–199.

Petrich, J. W., Lambry, J. C., Kuczera, K., Karplus, M., Poyart, C., & Martin, J. C. (1991) *Biochemistry 30*, 3975–3987.

Perutz, M. F., & Matthews, F. S. (1966) *J. Mol. Biol. 21*, 199–202.

Perutz, M. F., Fermi, G., Luisi, B., Shaanan, B., & Liddington, R. C. (1987) *Acc. Chem. Res. 20*, 309–321.

Petzold, L. R. (1983) *SIAM J. Sci. Stat. Comput. 4*, 136–148.

Phillips, S. E. V. (1980) *J. Mol. Biol. 142*, 531–554.

Press, W. H., Flannery, B. P., Teukolsky, S. A., & Vetterling, W. T. (1986) *Numerical Recipies: The Art of Scientific Computing*, Cambridge University Press, Cambridge.

Rasmussen, D. H., & MacKenzie, A. P. (1971) *J. Phys. Chem. 75*, 967–973.

Richard, L., Genberg, L., Deak, J., Chiu, H.-L., & Miller, R. J. D. (1992) *Biochemistry 31*, 10703–10715.

Rivetti, C., Mozzarelli, A., Rossi, G. L., Henry, E. R., & Eaton, W. A. (1993) *Biochemistry 32*, 2888–2906.

Sawicki, C. A., & Gibson, Q. H. (1976) *J. Biol. Chem. 251*, 1533–1542.

Schaad, O., Zhou, H.-X., Szabo, A., Eaton, W. A., & Henry, E. R. (1993) *Proc. Natl. Acad. Sci. U.S.A. 90*, 9547–9551.

Schomacker, K. T., & Champion, P. M. (1986) *J. Chem. Phys. 84*, 5314–5325.

Schuresco, D. D., & Webb, W. W. (1978) *Biophys. J. 24*, 382–383.

Shank, C. V., Ippen, E. P., & Bersohn, R. (1976) *Science 193*, 50–51.

Šrajer, V., & Champion, P. M. (1991) *Biochemistry 30*, 7390–7402.

Steinbach, P. J., Ansari, A., Berendzen, J., Braunstein, D., Chu, K., Cowen, B. R., Ehrenstein, D., Frauenfelder, H., Johnson, J. B., Lamb, D. C., Luck, S., Mourant, J. R., Nienhaus, G. U., Ormos, P., Philipp, R., Xie, A., & Young, R. D. (1991) *Biochemistry 30*, 3988–4001.

Tian, W. D., Sage, J. T., Šrajer, V., & Champion, P. M. (1992) *Phys. Rev. Lett. 68*, 408–411.

Traylor, T. G., Magde, D., Taube, D. J., Jongeward, K. A., Bandyopadhyay, D., Luo, J., & Walda, K. N. (1992) *J. Am. Chem. Soc. 114*, 417–429.

Westrick, J. A., & Peters, K. S. (1990) *Biophys. Chem. 37*, 73–79.

Westrick, J. A., Goodman, J. L., & Peters, K. S. (1987) *Biochemistry 26*, 8313–8318.

Xie, X., & Simon, J. D. (1991) *Biochemistry 30*, 3682–3692.

Young, R. D., Frauenfelder, H., Johnson, J. B., Lamb, D. C., Nienhaus, G. U., Philipp, R., & Scholl, R. (1991) *Chem. Phys. 158*, 315–327.

Zwanzig, R. (1992) *J. Chem. Phys. 97*, 3587–3589.